Hindawi
Mathematical Problems in Engineering
Volume 2022, Article ID 9360263, 23 pages
https://doi.org/10.1155/2022/9360263

Research Article

Dynamical Behaviors of Lumpoff and Rogue Wave Solutions for Nonlocal Gardner Equation

Jalil Manafian,[1,2] **Seyedeh Fatemeh Shahabi Takami**,[3] **Baharak Eslami**,[4] **Somaye Malmir**,[4] **Anju Sood**,[5] **and Amarpreet Kaur Sabherwal**[6,7]

[1]*Department of Applied Mathematics, Faculty of Mathematical Sciences, University of Tabriz, Tabriz, Iran*
[2]*Natural Sciences Faculty, Lankaran State University, 50, H. Aslanov Str., Lankaran, Azerbaijan*
[3]*Department of Mathematics, Pure Mathematics, Analytical Tendency, Iran University of Science and Technology, Narmak 16845, Tehran, Iran*
[4]*Department of Physics, Payame Noor University, P.O. Box 19395-3697, Tehran, Iran*
[5]*Department of Physical Sciences, Sant Baba Bhag Singh University, Jalandhar 144030, India*
[6]*Department of Mathematics, SGTB Khalsa College, University of Delhi, New Delhi 110007, India*
[7]*Sant Baba Bhag Singh University, Jalandhar, Punjab, India*

Correspondence should be addressed to Jalil Manafian; j_manafianheris@tabrizu.ac.ir

Received 16 June 2022; Accepted 21 September 2022; Published 14 October 2022

Academic Editor: Abdullahi Yusuf

In this paper, we got a novel kind of rogue waves with the predictability of $(2+1)$-dimensional nonlocal Gardner equation with the aid of Maple according to the Hirota bilinear model. We first construct a general quadratic function to derive the general lump solution for the mentioned equation. At the same time, the lumpoff solutions are demonstrated with more free autocephalous parameters, in which the lump solution is localized in all directions in space. Moreover, when the lump solution is cut by twin-solitons, special rogue waves are also introduced. Based on the data available in the literature, the resulting soliton solutions are innovative, developed, distinctive, and significant and can be applied to more complex phenomena, and they are immensely active for nonlinear models of classical and fractional-order type. To examine the dynamic behavior of the waves, contour 3D and 2D plots of several obtained findings are sketched by assigning specific values to the parameters. Furthermore, we obtain new sufficient solutions containing cross-kink, periodic-kink, multi-waves, and solitary wave solutions. It is worth noting that the emerging time and place of the rogue waves depend on the moving path of the lump solution.

1. Introduction

Nonlinear physical structures have been linked with nonlinear equations concerning several disciplines, like thermodynamics, mechanics, fluid dynamics, wave propagation, plasma physics, fluid flow, nonlinear networks, optical fibers, and soil consolidations, to develop vital phenomenon and implementations ([1–4])[5, 6]. The role of nonlinearity in waves is quite significant, mostly throughout non-linear sciences; research development towards exact solutions of partial differential nonlinear equations has always been a major endeavor for the past couple of years. All the while, several powerful, efficient, and reliable methods for attempting to seek exact analytical solutions to traveling waves have been established: for example, the N-soliton solution [7], a fractional-order multiple-model type-3 fuzzy control [8], a calculation methodology for geometrical characteristics [9], a combination of group method of data handling and computational fluid dynamics [10], the truss optimization with metaheuristic algorithms [11], the extended generalized Darboux method [12], the Lax pair technique [13], intermolecular interactions to the modern acid-base theory [14], the deep learning for Feynman's path integral [15], the Darboux–Bäcklund technique [16], the Hirota bilinear technique [17], the multiple exp-function method [18], optimal structure design [19], the experimental study on circular steel [20, 21], an influence of seismic orientation on the statistical distribution [22], effects of actual loading waveforms on the fatigue behaviors [23], and so on [24–27]. Hirota bilinear method is an efficient instrument to construct exact solutions of NLEEs, and there exist a lot of completely integrable equations that are investigated in this procedure, for example, the generalized bilinear equations [28], the Kadomtsev–Petviashvili (KP)–Benjamin–Bona–Mahony equation [29], the optimal Galerkin-homotopy asymptotic method [30], the $(2+1)$-dimensional generalized Calogero–Bogoyavlenskii–Schiff equation [31], the KP equation [32], the B-type KP equation [33], the optical interactions within magnetic layered structures [34], the $(2+1)$-dimensional breaking soliton equation [35], and the bidirectional Sawada–Kotera equation [36].

As we all know, the $(1+1)$-dimensional Gardner equation is an important equation and is a mixed version of the well-known Korteweg-De Vries (KdV) equation and the modified KdV (mKdV) equation [37, 38], and its properties are widely used in the field of mathematical physics, fluid dynamics, hydrodynamics, quantum mechanics, and nonlinear optics which is presented as follows:

$$u_t + 6\beta u u_x + u_{xxx} - \frac{3}{2}\alpha^2 u^2 u_x = 0, \tag{1}$$

the Gardner equation is completely integrable. The diverse kinds of exact solutions of Eq. (1) were studied by several techniques where interested researchers have worked on it, for example, using the inverse spectral transform method and constructing explicitly the exact solutions by the ∂-dressing method [39], utilizing the Casorati and Grammian determinant solutions to the $(2+1)$-dimensional Gardner equation [40], the tan h method with kink solutions [41], and the nonlinearization technique of Lax pairs to find the integrable decompositions for the $(2+1)$-dimensional Gardner [42]. Konopelchenko and Dubrovsky suggested the integro-differential form for the $(2+1)$-dimensional (D) Gardner equation as below:

$$\begin{aligned} &u_t + 6\beta u u_x + u_{xxx} - \frac{3}{2}\alpha^2 u^2 u_x + 3\sigma^2 \partial_x^{-1} u_{yy} \\ &\quad - 3\alpha\sigma u_x \partial_x^{-1} u_y = 0, \end{aligned} \tag{2}$$

where $\sigma^2 = \pm 1$, α and β are nonzero arbitrary values, and $u = u(x, y, t)$. Also, the operator $\partial_x^{-1}(.) = \int_0^x (.)$. All cases for parameters α, β, and σ have been investigated in the valuable works such as nonlocal symmetry and exact solutions [43], N-soliton solution and soliton resonances [44], and lie symmetries and invariant solutions [45] of $(2+1)$-dimensional Gardner equation.

Different kinds of probes were studied by proficient scholars in which many of them can be indicated, for instance, the generalized higher-order NLSE [46], the double dispersive equation in Murnaghan's rod [47], the fractional $(2+1)$-D Boussinesq dynamical model [48], the conformable time-fractional Wu-Zhang system [49], and the time-fractional model of Lassa hemorrhagic fever spreading [50]. In the valuable works, the important periodic and breather solutions to the KP-BBM equation [51] and generalized Bogoyavlensky–Konopelchenko equation [52] with the help of the Hirota technique were obtained. Authors of Reference [53] investigated the exact soliton solutions of a nonlinear Schrödinger equation including Kudryashov's sextic power-law nonlinearity by two efficient analytical methods. Cinar et al.[54] studied the soliton solutions for the perturbed Fokas–Lenells equation which has a vital role in optics by using Sardar subequation method. In Reference [55], the analytical solutions of simplified modified Camassa–Holm equations with various derivative operators, namely, conformable and M-truncated derivatives were obtained. Also, the analytical solutions of $(2+1)$ dimensional Heisenberg ferromagnetic spin equation which describes the nonlinear dynamics of the ferromagnetic materials by using the extended rational sine-cosine and sin h-cos h methods were reached [56]. The dark, singular, combined dark-singular soliton, singular periodic wave, and rational function solutions for the $(2+1)$-dimensional Biswas–Milovic equation for the description of pulse propagation in optical fiber were constructed [57]. Some authors worked on the nonlinear PDEs including the nonlinear directional couplers in nonlinear optics [58]; an improved perturbed Schrödinger equation with Kerr law nonlinearity in nonlinear optics [59]; the fractional analysis of fusion and fission process in plasma physics [60]; traveling, periodic, quasiperiodic, and chaotic structures of perturbed Fokas–Lenells model [61]; and dynamics of longitudinal bud equation among a magneto-electro-elastic round rod [62]. In Reference [63], the (G'/G)-expansion and the Ricatti transformation method were used for solving the $(2+1)$-dimensional Boussinesq equation. The analytical solutions to integer and fractional-order to KdV and Fornberg–Whitham equations were obtained by using the Laplace transforms, Sumudu transforms, and Elzaki transforms [64]. Scholars of Reference [65] studied Yang transform homotopy perturbation method to nonlinear fractional order KdV and Burger equation with exponential-decay kernel and provided formulae for the Yang transform of Caputo–Fabrizio fractional-order derivatives.

The lump, lumpoff, rogue wave, lump-periodic, periodic wave, cross-kink, multiwave, and solitary wave solutions of (2) will be investigated and analyzed. According to the Hirota bilinear model (2), the general periodic wave solution is concluded in Section 2 and also the new periodic solutions which can be arisen with more than five classes. Finally, conclusions are given is Section 10.

2. General Lump Solutions

According to Reference [66], the Hirota bilinear form of the Gardner equation is as follows:

$$\begin{aligned} &\left(\frac{2\sigma}{\alpha}D_y - \frac{2}{\alpha}D_x^2 - \frac{4\beta}{\alpha^2}D_x\right) g.f = 0, \\ &\left(D_x^3 + D_t + 3D_x D_y + \frac{6\sigma\beta}{\alpha}D_y\right) g.f = 0, \end{aligned} \tag{3}$$

under the condition of transformation:

$$u = -\frac{2}{\alpha}\left(\ln\frac{g}{f}\right)_x. \tag{4}$$

Here, the D-operator is defined as follows:

$$\begin{aligned} &D_x^a D_y^b D_t^c (F_1 \cdot F_2) \\ &= \left(\frac{\partial}{\partial x} - \frac{\partial}{\partial x'}\right)^a \left(\frac{\partial}{\partial y} - \frac{\partial}{\partial y'}\right)^b \left(\frac{\partial}{\partial t} - \frac{\partial}{\partial t'}\right)^c \\ &F_1(x, y, t) F_2(x', y', t')_{x=x', y=y', t=t'}. \end{aligned} \tag{5}$$

With the help of transformation (4), the general lump solutions of Eq. (3) can be given. We introduce ansatz f and g as follows:

$$f = x^T \Sigma x + f_0,\ g = x^T \Lambda x + g_0,\ 0. \tag{6}$$

with,

$$\begin{aligned} \Sigma &= \begin{pmatrix} \varepsilon_{00} & \varepsilon_{01} & \varepsilon_{02} & \varepsilon_{04} \\ \varepsilon_{10} & \varepsilon_{11} & \varepsilon_{12} & \varepsilon_{13} \\ \varepsilon_{20} & \varepsilon_{21} & \varepsilon_{22} & \varepsilon_{23} \\ \varepsilon_{30} & \varepsilon_{31} & \varepsilon_{32} & \varepsilon_{33} \end{pmatrix}, \\ \Lambda &= \begin{pmatrix} \lambda_{00} & \lambda_{01} & \lambda_{02} & \lambda_{04} \\ \lambda_{10} & \lambda_{11} & \lambda_{12} & \lambda_{13} \\ \lambda_{20} & \lambda_{21} & \lambda_{22} & \lambda_{23} \\ \lambda_{30} & \lambda_{31} & \lambda_{32} & \lambda_{33} \end{pmatrix}, \\ x^T &= (1, x, y, t), \end{aligned} \tag{7}$$

in which $\Sigma, \Lambda \in R^{4\times 4}$ are the symmetric matrixes and f_0 and g_0 are the positive constants. Then,

$$\begin{aligned} f &= \sum_{i\le j=0}^{3} \varepsilon_{ij} x_i x_j + f_0 \\ &= \varepsilon_{11}x^2 + \varepsilon_{22}y^2 + \varepsilon_{33}t^2 + 2\varepsilon_{12}xy + 2\varepsilon_{13}xt + 2\varepsilon_{23}yt \\ &\quad + 2\varepsilon_{01}x + \varepsilon_{02}y + 2\varepsilon_{03}t + \varepsilon_{00} + f_0, \\ g &= \sum_{i\le j=0}^{3} \lambda_{ij} x_i x_j + g_0 \\ &= \lambda_{11}x^2 + \lambda_{22}y^2 + \lambda_{33}t^2 + 2\lambda_{12}xy + 2\lambda_{13}xt + 2\lambda_{23}yt \\ &\quad + 2\lambda_{01}x + \lambda_{02}y + 2\lambda_{03}t + \lambda_{00} + g_0, \end{aligned} \tag{8}$$

or we can write the custom form as below:

$$\begin{aligned} f &= \delta_1(\varepsilon_1 x + \varepsilon_2 y + \varepsilon_3 t + \varepsilon_4)^2 \\ &\quad + \delta_2(\lambda_1 x + \lambda_2 y + \lambda_3 t + \lambda_4)^2 + \varepsilon_0, \\ g &= \delta_3(\varepsilon_1 x + \varepsilon_2 y + \varepsilon_3 t + \varepsilon_4)^2 \\ &\quad + \delta_4(\lambda_1 x + \lambda_2 y + \lambda_3 t + \lambda_4)^2 + \lambda_0. \end{aligned} \tag{9}$$

Substituting relations (10) and (11) into Eq. (3) and collecting all the coefficients of x, y, t, we can get twenty determining equations. Solving these resulting equations, we have the following cases:

Case 1.

$$\begin{aligned} \epsilon_2 &= -\frac{2}{3}\frac{\epsilon_1}{\alpha}, \\ \epsilon_3 &= \frac{4}{3}\frac{\epsilon_1(3\beta\sigma - 3\beta - \sigma)}{\alpha^2}, \\ \epsilon_4 &= -\frac{2}{3}\frac{\lambda_4\epsilon_1}{\lambda_2\alpha}, \\ \lambda_1 &= -\frac{3}{2}\lambda_2\alpha, \\ \lambda_3 &= -\frac{2(3\beta\sigma - 3\beta - \sigma)\lambda_2}{\alpha}. \end{aligned} \tag{10}$$

Under the transformation $u = -(2/\alpha)(\ln(g/f))_x$, the corresponding general lump solutions is read as follows:

$$u_{\text{lump}} = -\frac{2}{\alpha}\frac{g}{f}\left(\frac{(df/dx)}{g} - \frac{f(dg/dx)}{g^2}\right), \tag{11}$$

in which,

$$\begin{aligned} f &= \delta_1\left(\frac{4}{3}\frac{t\epsilon_1(3\beta\sigma - 3\beta - \sigma)}{\alpha^2} + x\epsilon_1 - \frac{2}{3}\frac{y\epsilon_1}{\alpha} - \frac{2}{3}\frac{\lambda_4\epsilon_1}{\lambda_2\alpha}\right)^2 \\ &\quad + \delta_2\left(-\frac{2t(3\beta\sigma - 3\beta - \sigma)\lambda_2}{\alpha} - \frac{3}{2}x\alpha\lambda_2 + y\lambda_2 + \lambda_4\right)^2 + \varepsilon_0, \\ g &= \delta_3\left(\frac{4}{3}\frac{t\epsilon_1(3\beta\sigma - 3\beta - \sigma)}{\alpha^2} + x\epsilon_1 - \frac{2}{3}\frac{y\epsilon_1}{\alpha} - \frac{2}{3}\frac{\lambda_4\epsilon_1}{\lambda_2\alpha}\right)^2 \\ &\quad + \delta_4\left(-\frac{2t(3\beta\sigma - 3\beta - \sigma)\lambda_2}{\alpha} - \frac{3}{2}x\alpha\lambda_2 + y\lambda_2 + \lambda_4\right)^2 + \lambda_0. \end{aligned} \tag{12}$$

Case 2.

$$\begin{aligned} \epsilon_0 &= \frac{\left(9\alpha^2\delta_2\lambda_2^2 + 4\delta_1\epsilon_1^2\right)\lambda_0}{9\alpha^2\delta_4\lambda_2^2 + 4\delta_3\epsilon_1^2}, \\ \epsilon_2 &= -\frac{2}{3}\frac{\epsilon_1}{\alpha}, \\ \epsilon_3 &= -\frac{2}{3}\frac{\epsilon_1\lambda_3}{\lambda_2\alpha}, \\ \epsilon_4 &= -\frac{2}{3}\frac{\lambda_4\epsilon_1}{\lambda_2\alpha}, \\ \lambda_1 &= -\frac{3}{2}\lambda_2\alpha. \end{aligned} \tag{13}$$

Under the transformation $u = -(2/\alpha)(\ln(g/f))_x$, the corresponding general lump solutions read as follows (see Figure 1):

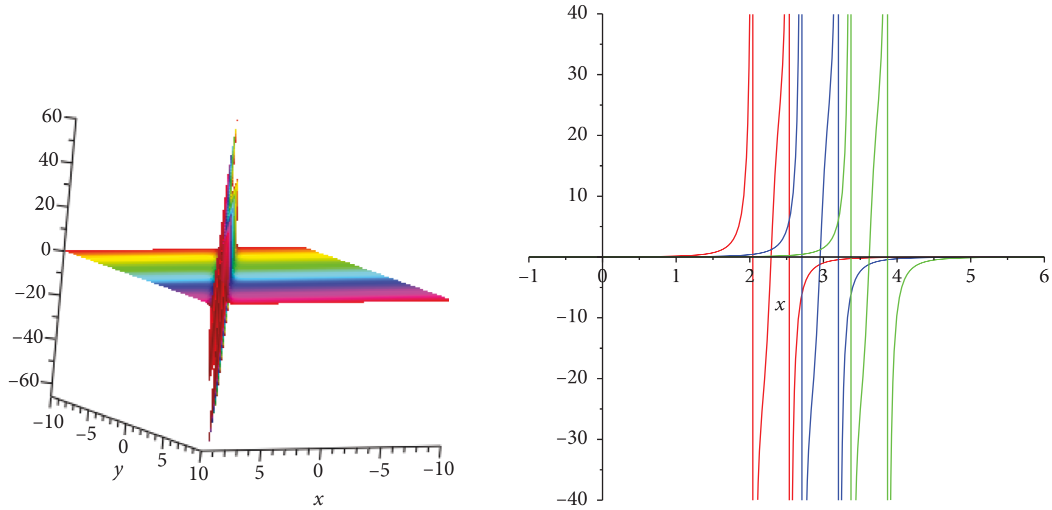

(f1) (f2)

Figure 1: Behavior of lump solution $u(x, y, t)$ in Eq. (13) with the selected amounts $\alpha = 1, \beta = 1, \sigma = 1, \epsilon_0 = 1, \epsilon_1 = 2, \lambda_0 = 2, \epsilon_1 = 2, \lambda_2 = 3, \lambda_4 = 1.3, \delta_1 = 1, \delta_2 = 2.5, \delta_3 = 2, \delta_4 = -2, t = 2$.

$$u_{\text{lump}} = -\frac{2}{\alpha}\frac{g}{f}\left(\frac{(\mathrm{d}f/\mathrm{d}x)}{g} - \frac{f(\mathrm{d}g/\mathrm{d}x)}{g^2}\right), \tag{14}$$

in which

$$\begin{aligned} f &= \delta_1\left(-\frac{2}{3}\frac{t\epsilon_1\lambda_3}{\lambda_2\alpha} + x\epsilon_1 - \frac{2}{3}\frac{y\epsilon_1}{\alpha} - \frac{2}{3}\frac{\lambda_4\epsilon_1}{\lambda_2\alpha}\right)^2 \\ &\quad + \delta_2\left(t\lambda_3 - \frac{3}{2}x\alpha\lambda_2 + y\lambda_2 + \lambda_4\right)^2 + \frac{\left(9\alpha^2\delta_2\lambda_2^2 + 4\delta_1\epsilon_1^2\right)\lambda_0}{9\alpha^2\delta_4\lambda_2^2 + 4\delta_3\epsilon_1^2}, \\ g &= \delta_3\left(-\frac{2}{3}\frac{t\epsilon_1\lambda_3}{\lambda_2\alpha} + x\epsilon_1 - \frac{2}{3}\frac{y\epsilon_1}{\alpha} - \frac{2}{3}\frac{\lambda_4\epsilon_1}{\lambda_2\alpha}\right)^2 \\ &\quad + \delta_4\left(t\lambda_3 - \frac{3}{2}x\alpha\lambda_2 + y\lambda_2 + \lambda_4\right)^2 + \lambda_0. \end{aligned} \tag{15}$$

3. Lumpoff Solution

In the section, the lumpoff solutions of the Gardner equation, a solution with the interaction between lump wave and stripe soliton wave, are investigated. On the basis of f_{lump} and g_{lump} of the general lump solutions, the lumpoff solutions can be written as follows:

$$\begin{aligned} f &= (\varepsilon_1 x + \varepsilon_2 y + \varepsilon_3 t + \varepsilon_4)^2 + (\lambda_1 x + \lambda_2 y + \lambda_3 t + \lambda_4)^2 \\ &\quad + \delta_1 e^{\theta_1 x + \theta_2 y + \theta_3 t + \theta_4} + \varepsilon_0, \end{aligned} \tag{16}$$

$$\begin{aligned} g &= (\varepsilon_1 x + \varepsilon_2 y + \varepsilon_3 t + \varepsilon_4)^2 + (\lambda_1 x + \lambda_2 y + \lambda_3 t + \lambda_4)^2 \\ &\quad + \delta_2 e^{\theta_1 x + \theta_2 y + \theta_3 t + \theta_4} + \lambda_0. \end{aligned} \tag{17}$$

We can easily detect that it consists of two parts: lump wave part and solitary wave part. It is worth noting that the solitary wave part is dominant when $\theta_1 x + \theta_2 y + \theta_3 t + \theta_4 > 0$. Otherwise, the lump solution only arises when $\theta_1 x + \theta_2 y + \theta_3 t + \theta_4 < 0$. To summarize, the existence of the soliton is based on the existence of the lump. Then, substituting (16) and (17) into Eq. (3), the selected constants of f_{lumpoff} and g_{lumpoff} are obtained as follows:

Case 3.

$$\begin{aligned} \epsilon_2 &= -\frac{2}{3}\frac{\epsilon_1}{\alpha}, \\ \epsilon_3 &= \frac{4}{3}\frac{\epsilon_1(3\beta\sigma - 3\beta - \sigma)}{\alpha^2}, \\ \lambda_1 &= -\frac{3}{2}\lambda_2\alpha, \\ \lambda_3 &= -\frac{2(3\beta\sigma - 3\beta - \sigma)\lambda_2}{\alpha}, \\ \theta_3 &= 2\frac{\sigma\theta_2(3\beta - 1)}{\alpha}. \end{aligned} \tag{18}$$

Under the transformation $u = -(2/\alpha)(\ln(g/f))_x$, the corresponding general lumpoff solutions read as follows:

$$\begin{aligned} u_{\text{lumpoff}} &= -\frac{2}{\alpha}\frac{g_{\text{lumpoff}}}{f_{\text{lumpoff}}} \\ &\quad \cdot \left(\frac{\left(\mathrm{d}f_{\text{lumpoff}}/\mathrm{d}x\right)}{g_{\text{lumpoff}}} - \frac{f_{\text{lumpoff}}\left(\mathrm{d}g_{\text{lumpoff}}/\mathrm{d}x\right)}{g_{\text{lumpoff}}^2}\right), \end{aligned} \tag{19}$$

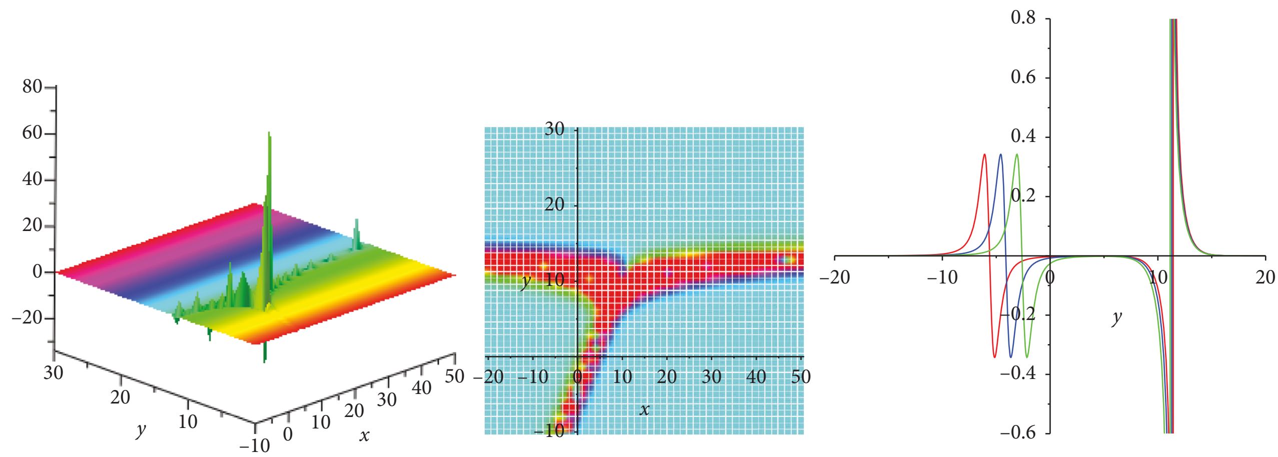

(f1) (f2) (f3)

Figure 2: Behavior of lumpoff solution $u(x,y,t)$ in Eq. (25) with the selected amounts $\alpha=1,\beta=1,\sigma=1,\epsilon_0=1,\epsilon_1=2,\lambda_0=2,\epsilon_1=2,$ $\lambda_2=3,\lambda_4=1.3,\delta_1=1,\delta_2=2.5,\delta_3=2,\delta_4=-2,\theta_2=1.5,\theta_4=2,t=2$.

in which,

$$
\begin{aligned}
f_{\text{lumpoff}} &= \left(\frac{4}{3}\frac{t\varepsilon_1(3\beta\sigma-3\beta-\sigma)}{\alpha^2}+x\varepsilon_1-\frac{2}{3}\frac{y\varepsilon_1}{\alpha}-\frac{2}{3}\frac{\lambda_4\varepsilon_1}{\lambda_2\alpha}\right)^2\\
&\quad+\left(-\frac{2t(3\beta\sigma-3\beta-\sigma)\lambda_2}{\alpha}-\frac{3}{2}x\alpha\lambda_2+y\lambda_2+\lambda_4\right)^2\\
&\quad-\delta_2 e^{-2(\sigma\theta_2(3\beta-1)t/\alpha)+y\theta_2+\theta_4}+\varepsilon_0,\\
g_{\text{lumpoff}} &= \delta_3\left(\frac{4}{3}\frac{t\varepsilon_1(3\beta\sigma-3\beta-\sigma)}{\alpha^2}+x\varepsilon_1-\frac{2}{3}\frac{y\varepsilon_1}{\alpha}-\frac{2}{3}\frac{\lambda_4\varepsilon_1}{\lambda_2\alpha}\right)^2\\
&\quad+\delta_4\left(-\frac{2t(3\beta\sigma-3\beta-\sigma)\lambda_2}{\alpha}-\frac{3}{2}x\alpha\lambda_2+y\lambda_2+\lambda_4\right)^2\\
&\quad+\delta_2 e^{-2(\sigma\theta_2(3\beta-1)t/\alpha)+y\theta_2+\theta_4}+\lambda_0.
\end{aligned}
\tag{20}
$$

Figure 2 presents the overtaking interactions between lump wave and stripe soliton wave containing 3D plot, density plot, and 2D plot, respectively, $(x=-1,0,1)$.

4. Rogue Waves with Predictability

In the section, we will explore the rogue waves with predictability for the $(2+1)$-dimensional Gardner equation. The so-called predictability is that the emerging time and place of the rogue waves can be described by some particular expressions. Let us consider a more general ansatz as follows:

$$
\begin{aligned}
f &= (\varepsilon_1 x+\varepsilon_2 y+\varepsilon_3 t+\varepsilon_4)^2+(\lambda_1 x+\lambda_2 y+\lambda_3 t+\lambda_4)^2\\
&\quad+\delta_1\cosh(\theta_1 x+\theta_2 y+\theta_3 t+\theta_4)+\varepsilon_0,
\end{aligned}
\tag{21}
$$

$$
\begin{aligned}
g &= (\varepsilon_1 x+\varepsilon_2 y+\varepsilon_3 t+\varepsilon_4)^2+(\lambda_1 x+\lambda_2 y+\lambda_3 t+\lambda_4)^2\\
&\quad+\delta_2\cosh(\theta_1 x+\theta_2 y+\theta_3 t+\theta_4)+\lambda_0.
\end{aligned}
\tag{22}
$$

Substituting (21) and (22) into Eq. (3) and collecting all relevant coefficients of x, y, t, cosh, and sinh, a series of equations have been obtained. Solving these equations, we have the following case:

Case 4.

$$
\begin{aligned}
\epsilon_2 &= -\frac{2}{3}\frac{\epsilon_1}{\alpha},\\
\epsilon_3 &= \frac{4}{3}\frac{\epsilon_1(3\beta\sigma-3\beta-\sigma)}{\alpha^2},\\
\lambda_1 &= -\frac{3}{2}\lambda_2\alpha,\\
\lambda_3 &= -\frac{2(3\beta\sigma-3\beta-\sigma)\lambda_2}{\alpha},\\
\theta_3 &= 2\frac{\sigma\theta_2(3\beta-1)}{\alpha}.
\end{aligned}
\tag{23}
$$

Under the transformation $u=-(2/\alpha)(\ln(g/f))_x$, the corresponding special rogue solution is read as follows:

$$
u_{\text{rogue}} = -\frac{2}{\alpha}\frac{g_{\text{rogue}}}{f_{\text{rogue}}}\left(\frac{(\mathrm{d}f_{\text{rogue}}/\mathrm{d}x)}{g_{\text{rogue}}}-\frac{f_{\text{rogue}}(\mathrm{d}g_{\text{rogue}}/\mathrm{d}x)}{g_{\text{rogue}}^2}\right),
\tag{24}
$$

in which,

$$f_{\text{rogue}} = \left(\frac{4}{3}\frac{t\varepsilon_1(3\beta\sigma-3\beta-\sigma)}{\alpha^2} + x\varepsilon_1 - \frac{2}{3}\frac{y\varepsilon_1}{\alpha} - \frac{2}{3}\frac{\lambda_4\varepsilon_1}{\lambda_2\alpha}\right)^2 + \left(-\frac{2t(3\beta\sigma-3\beta-\sigma)\lambda_2}{\alpha} - \frac{3}{2}x\alpha\lambda_2 + y\lambda_2 + \lambda_4\right)^2 - \delta_2 \cos h\left(-2\frac{\sigma\theta_2(3\beta-1)t}{\alpha} + y\theta_2 + \theta_4\right) + \varepsilon_0,$$

$$g_{\text{rogue}} = \delta_3\left(\frac{4}{3}\frac{t\int_1(3\beta\sigma-3\beta-\sigma)}{\alpha^2} + x\varepsilon_1 - \frac{2}{3}\frac{y\varepsilon_1}{\alpha} - \frac{2}{3}\frac{\lambda_4\varepsilon_1}{\lambda_2\alpha}\right)^2 + \delta_4\left(-\frac{2t(3\beta\sigma-3\beta-\sigma)\lambda_2}{\alpha} - \frac{3}{2}x\alpha\lambda_2 + y\lambda_2 + \lambda_4\right)^2 + \delta_2 \cos h\left(-2\frac{\sigma\theta_2(3\beta-1)t}{\alpha} + y\theta_2 + \theta_4\right) + \lambda_0. \quad (25)$$

Actually, the hyperbolic function cos h part that predominates in f_{rogue} and g_{rogue} led to the lump waves which are always disappeared. Figure 3 presents the overtaking interactions between lump wave and stripe soliton wave containing 3D plot, density plot, and 2D plot, respectively, $(x = -1, 0, 1)$.

5. Lump-Periodic Solutions

In the section, we will explore the lump-periodic solutions for the $(2+1)$-dimensional Gardner equation. Let us consider a more general ansatz as follows:

$$f = (\varepsilon_1 x + \varepsilon_2 y + \varepsilon_3 t + \varepsilon_4)^2 + (\lambda_1 x + \lambda_2 y + \lambda_3 t + \lambda_4)^2 + \delta_1 \cos(\theta_1 x + \theta_2 y + \theta_3 t + \theta_4) + \varepsilon_0, \quad (26)$$

$$g = (\varepsilon_1 x + \varepsilon_2 y + \varepsilon_3 t + \varepsilon_4)^2 + (\lambda_1 x + \lambda_2 y + \lambda_3 t + \lambda_4)^2 + \delta_2 \cos(\theta_1 x + \theta_2 y + \theta_3 t + \theta_4) + \lambda_0. \quad (27)$$

Substituting (26) and (27) into Eq. (3) and collecting all relevant coefficients of x, y, t, cos, and sin, a series of equations have been obtained. Solving these equations, we have the following case:

Case 5.

$$\begin{aligned}
\epsilon_2 &= -\frac{2}{3}\frac{\epsilon_1}{\alpha},\\
\epsilon_3 &= \frac{4}{3}\frac{\epsilon_1(3\beta\sigma-3\beta-\sigma)}{\alpha^2},\\
\lambda_1 &= -\frac{3}{2}\lambda_2\alpha,\\
\lambda_3 &= -\frac{2(3\beta\sigma-3\beta-\sigma)\lambda_2}{\alpha},\\
\theta_3 &= -\frac{1}{8}\frac{\theta_2\left(27\alpha^4\theta_2^2+48\beta\sigma-48\beta-16\sigma\right)}{\alpha}.
\end{aligned} \quad (28)$$

Under the transformation $u = -(2/\alpha)(\ln(g/f))_x$, the corresponding special lump-periodic solution can be read as follows:

$$u_{LP} = -\frac{2}{\alpha}\frac{g_{LP}}{f_{LP}}\left(\frac{(\mathrm{d}f_{LP}/\mathrm{d}x)}{g_{LP}} - \frac{f_{LP}(\mathrm{d}g_{LP}/\mathrm{d}x)}{g_{LP}^2}\right), \quad (29)$$

in which,

$$\begin{aligned}
f_{LP} &= \left(\frac{4}{3}\frac{t\epsilon_1(3\beta\sigma-3\beta-\sigma)}{\alpha^2} + x\epsilon_1 - \frac{2}{3}\frac{y\epsilon_1}{\alpha} - \frac{2}{3}\frac{\lambda_4\epsilon_1}{\lambda_2\alpha}\right)^2 + \left(-\frac{2t(3\beta\sigma-3\beta-\sigma)\lambda_2}{\alpha} - \frac{3}{2}x\alpha\lambda_2 + y\lambda_2 + \lambda_4\right)^2\\
&\quad + \delta_2\cos\left(-\frac{1}{8}\frac{\theta_2\left(27\alpha^4\theta_2^2+48\beta\sigma-48\beta-16\sigma\right)t}{\alpha} - \frac{3}{2}x\alpha\theta_2 + y\theta_2 + \theta_4\right) + \varepsilon_0,\\
g_{LP} &= \delta_3\left(\frac{4}{3}\frac{t\epsilon_1(3\beta\sigma-3\beta-\sigma)}{\alpha^2} + x\epsilon_1 - \frac{2}{3}\frac{y\epsilon_1}{\alpha} - \frac{2}{3}\frac{\lambda_4\epsilon_1}{\lambda_2\alpha}\right)^2 + \delta_4\left(-\frac{2t(3\beta\sigma-3\beta-\sigma)\lambda_2}{\alpha} - \frac{3}{2}x\alpha\lambda_2 + y\lambda_2 + \lambda_4\right)^2\\
&\quad + \delta_2\cos\left(-\frac{1}{8}\frac{\theta_2\left(27\alpha^4\theta_2^2+48\beta\sigma-48\beta-16\sigma\right)t}{\alpha} - \frac{3}{2}x\alpha\theta_2 + y\theta_2 + \theta_4\right) + \lambda_0.
\end{aligned} \quad (30)$$

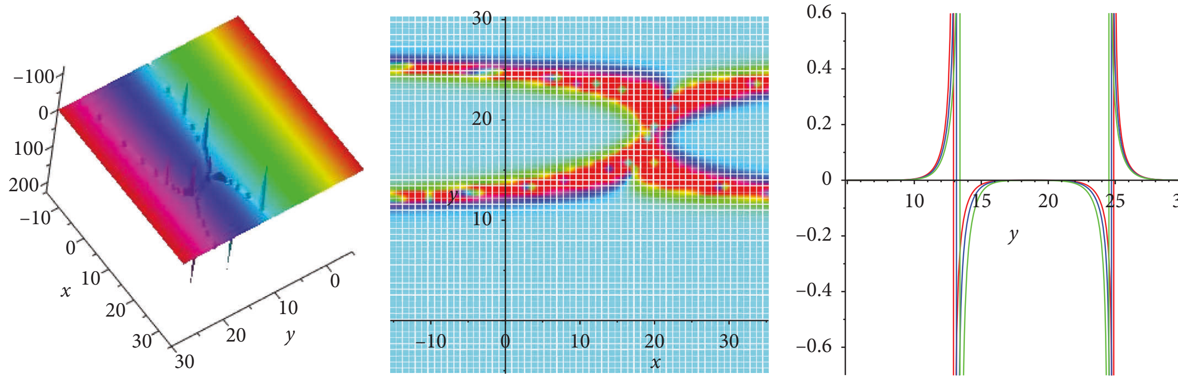

(f1) (f2) (f3)

Figure 3: Behavior of rogue wave solution for I and II and singular solution for III of $u(x, y, t)$ in Eq. (31) with the selected amounts $\alpha = 1, \beta = 1, \sigma = 1, \epsilon_0 = 1, \epsilon_1 = 2, \lambda_0 = 2, \epsilon_1 = 2, \lambda_2 = 3, \lambda_4 = 1.3, \delta_1 = 1, \delta_2 = 2.5, \delta_3 = 2, \delta_4 = -2, \theta_2 = 1.5, \theta_4 = 2, t = 2$.

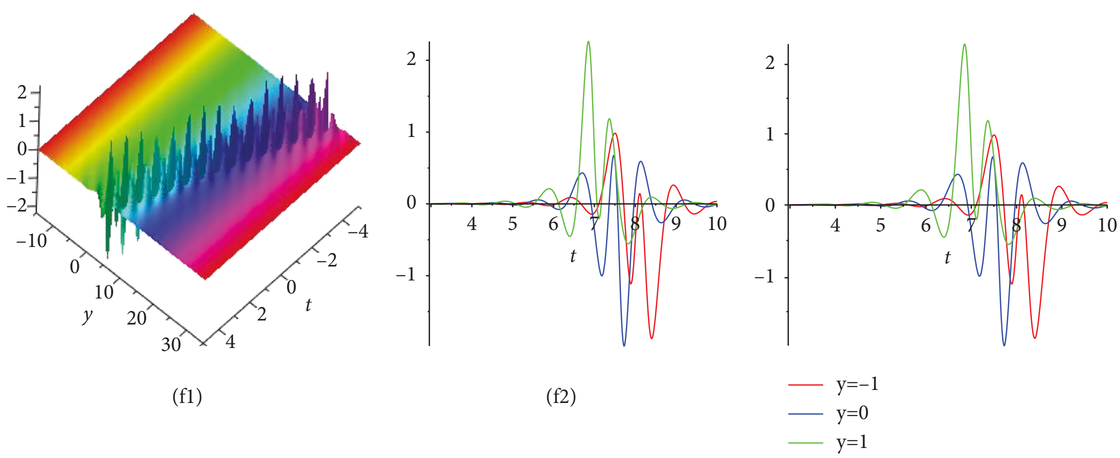

(f1) (f2) (f3)

Figure 4: Behavior of lump-periodic solution $u(x, y, t)$ in Eq. (37) with the selected amounts $\alpha = 1, \beta = 1, \sigma = 1, \epsilon_0 = 1, \epsilon_1 = 2, \lambda_0 = 2, \epsilon_1 = 2, \lambda_2 = 3, \lambda_4 = 1.3, \delta_1 = 1, \delta_2 = 2.5, \delta_3 = 2, \delta_4 = -2, \theta_2 = 1.5, \theta_4 = 2, t = 2$.

Figure 4 presents the overtaking interactions between lump wave and periodic wave containing 3D plot, density plot, and 2D plot, respectively, $(x = -1, 0, 1)$.

6. Double Breather Solutions

In the section, we will explore the breather solutions for the $(2+1)$-dimensional Gardner equation. Let us consider a more general ansatz as follows:

$$\begin{aligned} f = {} & e^{-\varepsilon_1 x - \varepsilon_2 y - \varepsilon_3 t - \varepsilon_4} + \delta_1 e^{\varepsilon_1 x + \varepsilon_2 y + \varepsilon_3 t + \varepsilon_4} \\ & + \delta_2 \sin(\lambda_1 x + \lambda_2 y + \lambda_3 t + \lambda_4) \\ & + \delta_3 \sin(2\lambda_1 x + 2\lambda_2 y + 2\lambda_3 t + 2\lambda_4), \end{aligned} \tag{31}$$

$$\begin{aligned} g = {} & e^{-\varepsilon_1 x - \varepsilon_2 y - \varepsilon_3 t - \varepsilon_4} + \delta_4 e^{\varepsilon_1 x + \varepsilon_2 y + \varepsilon_3 t + \varepsilon_4} \\ & + \delta_5 \sin(\lambda_1 x + \lambda_2 y + \lambda_3 t + \lambda_4) \\ & + \delta_6 \sin(2\lambda_1 x + 2\lambda_2 y + 2\lambda_3 t + 2\lambda_4). \end{aligned} \tag{32}$$

Substituting (31) and (32) into Eq. (3) and collecting all relevant coefficients of exp, cos, and sin, a series of equations have been obtained. Solving these equations, we have the following case:

Case 6.

$$\begin{aligned} \epsilon_3 &= -\frac{\alpha^2 \epsilon_1^3 - 3\alpha^2 \epsilon_1 \epsilon_2 + 6\alpha\beta\sigma\epsilon_2 - 2\alpha\sigma\epsilon_2 - 2\alpha\epsilon_1^2 + 4\beta\epsilon_1}{\alpha^2}, \\ \lambda_3 &= \frac{\lambda_2 (3\alpha\epsilon_1 - 6\beta\sigma + 2\sigma)}{\alpha}. \end{aligned} \tag{33}$$

Under the transformation $u = -(2/\alpha)(\ln(g/f))_x$, the corresponding special breather solution is read as follows:

$$u_B = -\frac{2}{\alpha} \frac{g_B}{f_B} \left(\frac{(df_B/dx)}{g_B} - \frac{f_B (dg_B/dx)}{g_B^2} \right), \tag{34}$$

in which,

$$f_B = e^{-\Omega} + \delta_2 \sin(\Xi) + \delta_3 \sin(2\Xi), g_B = e^{-\Omega},$$

$$\Omega = \frac{t\left(\alpha^2\varepsilon_1^3 - 3\alpha^2\varepsilon_1\varepsilon_2 + 6\alpha\beta\sigma\varepsilon_2 - 2\alpha\sigma\varepsilon_2 - 2\alpha\varepsilon_1^2 + 4\beta\varepsilon_1\right)}{\alpha^2} - x\varepsilon_1 - y\varepsilon_2 - \varepsilon_4,$$

$$\Xi = \frac{\lambda_2\left(3\alpha\int_1 - 6\beta\sigma + 2\sigma\right)t}{\alpha} + \lambda_2 y + \lambda_4. \tag{35}$$

Figure 5 presents the overtaking interactions between stripe wave and periodic wave containing 3D plot, density plot, and 2D plot, respectively, $(y = -1, 0, 1)$.

Case 7.

$$\delta_1 = \frac{\delta_3^2\delta_4}{\delta_6^2},$$

$$\delta_2 = \frac{\delta_5\delta_3}{\delta_6},$$

$$\epsilon_2 = \frac{1}{3}\frac{\epsilon_1(3\alpha\delta_3\epsilon_1 + 3\alpha\delta_6\epsilon_1 - 2\delta_3 + 2\delta_6)}{\alpha(\delta_3 - \delta_6)},$$

$$\epsilon_3 = \frac{2}{3}\frac{\epsilon_1\omega}{(\delta_3 - \delta_6)^2\alpha^2},$$

$$\lambda_3 = \frac{\lambda_2(3\alpha\delta_3\epsilon_1 + 3\alpha\delta_6\epsilon_1 - 6\beta\sigma\delta_3 + 6\beta\sigma\delta_6 + 2\sigma\delta_3 - 2\sigma\delta_6)}{\alpha(\delta_3 - \delta_6)},$$

$$\omega = 3\alpha^2\delta_3^2\epsilon_1^2 + 12\alpha^2\delta_3\delta_6\epsilon_1^2 + 3\alpha^2\delta_6^2\epsilon_1^2 - 9\alpha\beta\sigma\delta_3^2\epsilon_1 + 9\alpha\beta\sigma\delta_6^2\epsilon_1 + 3\alpha\sigma\delta_3^2\epsilon_1 - 3\alpha\sigma\delta_6^2\epsilon_1 + 6\beta\sigma\delta_3^2 - 12\beta\sigma\delta_3\delta_6 + 6\beta\sigma\delta_6^2 - 6\beta\delta_3^2 + 12\beta\delta_3\delta_6 - 6\beta\delta_6^2 - 2\sigma\delta_3^2 + 4\sigma\delta_3\delta_6 - 2\sigma\delta_6^2. \tag{36}$$

Under the transformation $u = -(2/\alpha)(\ln(g/f))_x$, the corresponding special breather solution is read as follows:

$$u_B = -\frac{2}{\alpha}\frac{g_B}{f_B}\left(\frac{(\mathrm{d}f_B/\mathrm{d}x)}{g_B} - \frac{f_B(\mathrm{d}g_B/\mathrm{d}x)}{g_B^2}\right), \tag{37}$$

in which,

$$f_B = e^{-\Omega} + \frac{\delta_3^2\delta_4}{\delta_6^2}e^{\Omega} + \frac{\delta_5\delta_3}{\delta_6}\sin(\Xi) + \delta_3\sin(2\Xi),$$

$$g_B = e^{-\Omega} + \delta_4 e^{\Omega} + \delta_5\sin(\Xi) + \delta_6\sin(2\Xi),$$

$$\Omega = \frac{2}{3}\frac{t\varepsilon_1\omega}{(\delta_3 - \delta_6)^2\alpha^2} + x\varepsilon_1 + \frac{1}{3}\frac{y\varepsilon_1(3\alpha\delta_3\varepsilon_1 + 3\alpha\delta_6\varepsilon_1 - 2\delta_3 + 2\delta_6)}{\alpha(\delta_3 - \delta_6)} + \varepsilon_4,$$

$$\Xi = \frac{\lambda_2(3\alpha\delta_3\varepsilon_1 + 3\alpha\delta_6\varepsilon_1 - 6\beta\sigma\delta_3 + 6\beta\sigma\delta_6 + 2\sigma\delta_3 - 2\sigma\delta_6)t}{\alpha(\delta_3 - \delta_6)} + \lambda_2 y + \lambda_4. \tag{38}$$

Figure 6 presents the overtaking interactions between stripe wave and periodic wave containing 3D plot, density plot, and 2D plot, respectively, $(y = -1, 0, 1)$.

Case 8.

$$\delta_1 = \frac{\delta_3^3\delta_6}{(\delta_3 + \delta_6)^2},$$

$$\delta_4 = \frac{\delta_3\delta_6^3}{(\delta_3 + \delta_6)^2},$$

$$\epsilon_3 = -4\frac{\lambda_1(3\alpha\delta_3\lambda_2 + 3\alpha\delta_6\lambda_2 + 2\delta_3\lambda_1 + 2\delta_6\lambda_1)}{\alpha(\delta_3 - \delta_6)},$$

$$\lambda_3 = 2\frac{2\alpha^2\lambda_1^3 - 3\alpha\beta\sigma\lambda_2 + \alpha\sigma\lambda_2 - 2\beta\lambda_1}{\alpha^2}. \tag{39}$$

Under the transformation $u = -(2/\alpha)(\ln(g/f))_x$, the corresponding special breather solution is read as follows:

$$u_B = -\frac{2}{\alpha}\frac{g_B}{f_B}\left(\frac{(\mathrm{d}f_B/\mathrm{d}x)}{g_B} - \frac{f_B(\mathrm{d}g_B/\mathrm{d}x)}{g_B^2}\right), \tag{40}$$

in which,

$$f_B = e^{-\Omega} + \frac{\delta_3^2\delta_4}{\delta_6^2}e^{\Omega} + \delta_3\sin(2\Xi),$$

$$g_B = e^{-\Omega} + \delta_4 e^{\Omega} + \delta_6\sin(2\Xi),$$

$$\Omega = 4\frac{t\lambda_1(3\alpha\delta_3\lambda_2 + 3\alpha\delta_6\lambda_2 + 2\delta_3\lambda_1 + 2\delta_6\lambda_1)}{\alpha(\delta_3 - \delta_6)},$$

$$\Xi = 2\frac{\left(2\alpha^2\lambda_1^3 - 3\alpha\beta\sigma\lambda_2 + \alpha\sigma\lambda_2 - 2\beta\lambda_1\right)t}{\alpha^2} + \lambda_1 x + \lambda_2 y + \lambda_4. \tag{41}$$

Figure 7 presents the overtaking interactions between stripe wave and periodic wave containing 3D plot, density plot, and 2D plot, respectively, $(t = -0.01, 0, 0.01)$.

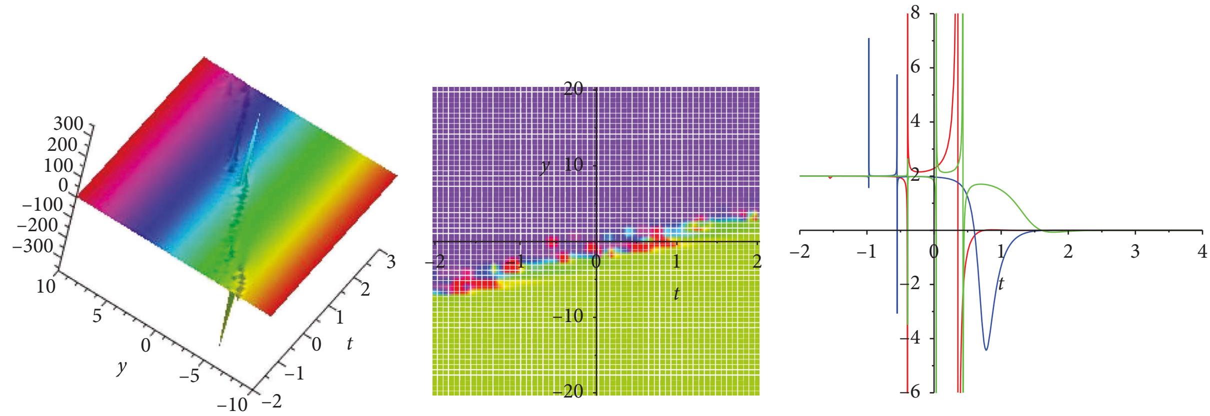

(f1) (f2) (f3)

Figure 5: Behavior of breather solution $u(x, y, t)$ in Eq. (43) with the selected amounts $\alpha = 1, \beta = 1, \sigma = 1, \epsilon_1 = 1, \epsilon_2 = 2, \epsilon_4 = 1.5, \lambda_2 = 2, \lambda_4 = 1.2, \delta_1 = 1.3, \delta_2 = 2, \delta_3 = 1.5, \delta_4 = 3, x = 1.5$.

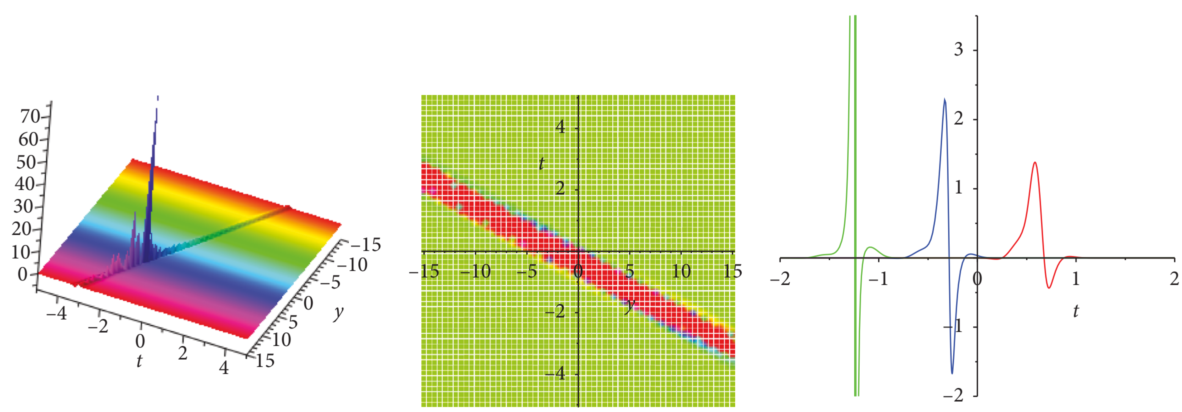

(f1) (f2) (f3)

Figure 6: Behavior of breather solution $u(x, y, t)$ in Eq. (45) with the selected amounts $\alpha = 1, \beta = 1, \sigma = 1, \epsilon_1 = 1, \epsilon_2 = 2, \epsilon_4 = 1.5, \lambda_2 = 2, \lambda_4 = 1.2, \delta_1 = 1.3, \delta_2 = 2, \delta_3 = 1.5, \delta_4 = 3, x = 1.5$.

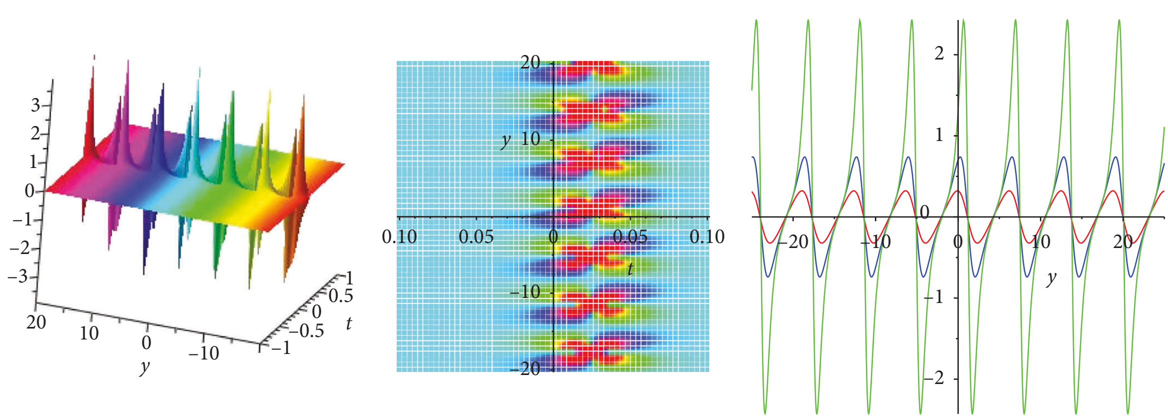

(f1) (f2) (f3)

Figure 7: Behavior of breather solution $u(x, y, t)$ in Eq. (49) with the selected amounts $\alpha = 1, \beta = 1, \sigma = 1, \epsilon_1 = 1, \epsilon_2 = 2, \epsilon_4 = 1.5, \lambda_2 = 2, \lambda_4 = 1.2, \delta_1 = 1.3, \delta_2 = 2, \delta_3 = 1.5, \delta_4 = 3, x = 1.5$.

7. Periodic Cross-Kink Solutions

In the section, we will explore the periodic cross-kink solutions for the $(2+1)$-dimensional Gardner equation. Let us consider a more general ansatz as follows:

$$f = e^{-\varepsilon_1 x-\varepsilon_2 y-\varepsilon_3 t-\varepsilon_4} + \delta_1 e^{\varepsilon_1 x+\varepsilon_2 y+\varepsilon_3 t+\varepsilon_4} + \delta_2 \sin\left(\lambda_1 x + \lambda_2 y + \lambda_3 t + \lambda_4\right) + \delta_3 \sinh\left(2\lambda_1 x + 2\lambda_2 y + 2\lambda_3 t + 2\lambda_4\right), \tag{42}$$

$$g = e^{-\varepsilon_1 x-\varepsilon_2 y-\varepsilon_3 t-\varepsilon_4} + \delta_4 e^{\varepsilon_1 x+\varepsilon_2 y+\varepsilon_3 t+\varepsilon_4} + \delta_5 \sin\left(\lambda_1 x + \lambda_2 y + \lambda_3 t + \lambda_4\right) + \delta_6 \sinh\left(2\lambda_1 x + 2\lambda_2 y + 2\lambda_3 t + 2\lambda_4\right). \tag{43}$$

Substituting (42) and (43) into Eq. (3) and collecting all relevant coefficients of exp, cos, sin, cosh, and sinh, a series of equations have been obtained. Solving these equations, we have the following cases:

Case 9.

$$\begin{aligned}
\epsilon_3 &= -\frac{\alpha^2\epsilon_1^3 - 3\alpha^2\epsilon_1\epsilon_2 + 6\alpha\beta\sigma\epsilon_2 - 2\alpha\sigma\epsilon_2 - 2\alpha\epsilon_1^2 + 4\beta\epsilon_1}{\alpha^2},\\
\lambda_3 &= -\frac{1}{3}\frac{\omega}{\alpha^2\delta_5^2\lambda_1},\\
\lambda_2 &= -\frac{1}{3}\frac{3\alpha\delta_6^2\epsilon_1\epsilon_2 + 12\alpha\delta_4\epsilon_1\epsilon_2 + 2\delta_5^2\lambda_1^2 + 2\delta_6^2\epsilon_1^2 + 8\delta_4\epsilon_1^2}{\alpha\delta_5^2\lambda_1},\\
\theta_2 &= -\frac{1}{3}\frac{3\alpha\epsilon_2 + 4\epsilon_1}{\alpha},\\
\omega &= 9\alpha^2\delta_5^2\epsilon_1^2\lambda_1^2 - 3\alpha^2\delta_5^2\lambda_1^4 - 18\alpha\beta\sigma\delta_6^2\epsilon_1\epsilon_2 - 72\alpha\beta\sigma\delta_4\epsilon_1\epsilon_2 + 6\alpha\sigma\delta_6^2\epsilon_1\epsilon_2 - 12\beta\sigma\delta_5^2\lambda_1^2\\
&\quad - 12\beta\sigma\delta_6^2\epsilon_1^2 + 24\alpha\sigma\delta_4\epsilon_1\epsilon_2 - 48\beta\sigma\delta_4\epsilon_1^2 + 12\beta\delta_5^2\lambda_1^2 + 4\sigma\delta_5^2\lambda_1^2 + 4\sigma\delta_6^2\epsilon_1^2 + 16\sigma\delta_4\epsilon_1^2.
\end{aligned} \tag{44}$$

Under the transformation $u = -(2/\alpha)(\ln(g/f))_x$, the corresponding special periodic cross-kink solution is read as follows:

$$u_{CK} = -\frac{2}{\alpha}\frac{g_{CK}}{f_{CK}}\left(\frac{(\mathrm{d}f_{CK}/\mathrm{d}x)}{g_{CK}} - \frac{f_{CK}(\mathrm{d}g_{CK}/\mathrm{d}x)}{g_{CK}^2}\right), \tag{45}$$

in which,

$$\begin{aligned}
f_{CK} &= e^{-\Omega} + \delta_4 e^{\Omega} - \delta_5 \sin(\Xi) + \delta_3 \sin h(\Lambda),\\
g_{CK} &= e^{-\Omega} + \delta_4 e^{\Omega} + \delta_5 \sin(\Xi) + \delta_3 \sin h(\Lambda),\\
\Omega &= -\frac{t\left(\alpha^2 \int_1^3 - 3\alpha^2 \int_1 \lambda_1^2 + 6\alpha\beta\sigma \int_2 - 2\alpha\sigma \int_2 + 4\beta \int_1\right)}{\alpha^2} + x\varepsilon_1 + y\varepsilon_2 + \varepsilon_4,\\
\Xi &= -\frac{1}{3}\frac{\omega t}{\alpha^2\delta_5^2\lambda_1} + \lambda_1 x - \frac{1}{3}\frac{y\left(3\alpha\delta_6^2\varepsilon_1\varepsilon_2 + 12\alpha\delta_4\varepsilon_1\varepsilon_2 + 2\delta_5^2\lambda_1^2 + 2\delta_6^2\varepsilon_1^2 + 8\delta_4\varepsilon_1^2\right)}{\alpha\delta_5^2\lambda_1} + \lambda_4,\\
\Lambda &= -\frac{1}{3}\frac{\left(3\alpha^2\varepsilon_1^3 - 9\alpha^2\varepsilon_1\lambda_1^2 - 18\alpha\beta\sigma\varepsilon_2 + 6\alpha\sigma\varepsilon_2 - 24\beta\sigma\varepsilon_1 + 12\beta\varepsilon_1 + 8\sigma\varepsilon_1\right)t}{\alpha^2} + x\int_1 - \frac{1}{3}\frac{y\left(3\alpha\varepsilon_2 + 4\varepsilon_1\right)}{\alpha} + \theta_4.
\end{aligned} \tag{46}$$

Case 10. .

$$u_{CK} = -\frac{2}{\alpha}\frac{g_{CK}}{f_{CK}}\left(\frac{(\mathrm{d}f_{CK}/\mathrm{d}x)}{g_{CK}} - \frac{f_{CK}(\mathrm{d}g_{CK}/\mathrm{d}x)}{g_{CK}^2}\right), \quad (47)$$

in which,

$$\begin{aligned}
f_{CK} &= e^{-\Omega} - \frac{1}{4}\delta_6^2 e^{\Omega} - \delta_5\sin(\Xi) + \delta_6\sin h(\Lambda),\\
g_{CK} &= e^{-\Omega} - \frac{1}{4}\delta_6^2 e^{\Omega} + \delta_5\sin(\Xi) + \delta_6\sin h(\Lambda),\\
\Omega &= -\frac{t\left(\alpha^2\int_1^3 + 6\alpha\beta\sigma\int_2 - 2\alpha\sigma\int_2 + 4\beta\int_1\right)}{\alpha^2} + x\varepsilon_1 + y\varepsilon_2 + \varepsilon_4,\\
\Xi &= -2\frac{\sigma\lambda_2(3\beta-1)t}{\alpha} + \lambda_2 y + \lambda_4,\\
\Lambda &= -\frac{1}{3}\frac{\left(3\alpha^2\varepsilon_1^3 - 18\alpha\beta\sigma\varepsilon_2 + 6\alpha\sigma\varepsilon_2 - 24\beta\sigma\varepsilon_1 + 12\beta\varepsilon_1 + 8\sigma\varepsilon_1\right)t}{\alpha^2}\\
&\quad + x\int_1 - \frac{1}{3}\frac{y\left(3\alpha\int_2 + 4\int_1\right)}{\alpha} + \theta_4.
\end{aligned} \quad (48)$$

Case 11.

$$u_{CK} = -\frac{2}{\alpha}\frac{g_{CK}}{f_{CK}}\left(\frac{(\mathrm{d}f_{CK}/\mathrm{d}x)}{g_{CK}} - \frac{f_{CK}(\mathrm{d}g_{CK}/\mathrm{d}x)}{g_{CK}^2}\right), \quad (49)$$

in which,

$$\begin{aligned}
f_{CK} &= e^{-\Omega} + \delta_4 e^{\Omega} - \delta_5\sin(\Xi) + \delta_6\sin h(\Lambda),\\
g_{CK} &= e^{-\Omega} + \delta_4 e^{\Omega} + \delta_5\sin(\Xi) + \delta_6\sin h(\Lambda),\\
\Omega &= -\frac{1}{3}\frac{t\varepsilon_1\left(3\alpha^2\varepsilon_1^2 - 12\beta\sigma + 12\beta + 4\sigma\right)}{\alpha^2}\\
&\quad + x\varepsilon_1 - \frac{2}{3}\frac{y\varepsilon_1}{\alpha} + \varepsilon_4,\\
\Xi &= -2\frac{\sigma\lambda_2(3\beta-1)t}{\alpha} + \lambda_2 y + \lambda_4,\\
\Lambda &= -\frac{1}{3}\frac{t\int_1\left(3\alpha^2\varepsilon_1^2 - 12\beta\sigma + 12\beta + 4\sigma\right)}{\alpha^2}\\
&\quad + x\varepsilon_1 - \frac{2}{3}\frac{y\varepsilon_1}{\alpha} + \theta_4.
\end{aligned} \quad (50)$$

Case 12.

$$u_{CK} = -\frac{2}{\alpha}\frac{g_{CK}}{f_{CK}}\left(\frac{(df_{CK}/dx)}{g_{CK}} - \frac{f_{CK}(dg_{CK}/dx)}{g_{CK}^2}\right), \quad (51)$$

in which,

$$\begin{aligned}
f_{CK} &= e^{-\Omega} + \delta_4 e^{\Omega} + \delta_2\sin(\Xi) + \delta_6\sin h(\Lambda),\\
g_{CK} &= e^{-\Omega} + \delta_4 e^{\Omega} + \delta_5\sin(\Xi) + \delta_6\sin h(\Lambda),\\
\Omega &= -\frac{1}{3}\frac{t\varepsilon_1\left(3\alpha^2\varepsilon_1^2 - 9\alpha^2\lambda_1^2 - 12\beta\sigma + 12\beta + 4\sigma\right)}{\alpha^2}\\
&\quad + x\varepsilon_1 - \frac{2}{3}\frac{y\varepsilon_1}{\alpha} + \varepsilon_4,\\
\Xi &= -\frac{1}{3}\frac{\left(9\alpha^2\varepsilon_1^2 - 3\alpha^2\lambda_1^2 - 12\beta\sigma + 12\beta + 4\sigma\right)\lambda_1 t}{\alpha^2}\\
&\quad + \lambda_1 x - \frac{2}{3}\frac{y\lambda_1}{\alpha} + \lambda_4,\\
\Lambda &= -\frac{1}{3}\frac{t\int_1\left(3\alpha^2\varepsilon_1^2 - 9\alpha^2\lambda_1^2 - 12\beta\sigma + 12\beta + 4\sigma\right)}{\alpha^2}\\
&\quad + x\varepsilon_1 - \frac{2}{3}\frac{y\varepsilon_1}{\alpha} + \theta_4.
\end{aligned} \quad (52)$$

Case 13.

$$u_{CK} = -\frac{2}{\alpha}\frac{g_{CK}}{f_{CK}}\left(\frac{(\mathrm{d}f_{CK}/\mathrm{d}x)}{g_{CK}} - \frac{f_{CK}(\mathrm{d}g_{CK}/\mathrm{d}x)}{g_{CK}^2}\right), \quad (53)$$

in which,

$$\begin{aligned}
f_{CK} &= e^{-\Omega} + \delta_2\sin(\Xi) + \delta_6\sin h(\Lambda),\\
g_{CK} &= e^{-\Omega} + \delta_5\sin(\Xi) + \delta_6\sin h(\Lambda),\\
\Omega &= \frac{1}{12}\frac{t\varepsilon_1\left(81\alpha^4\lambda_2^2 - 12\alpha^2\varepsilon_1^2 + 48\beta\sigma - 48\beta - 16\sigma\right)}{\alpha^2}\\
&\quad + x\varepsilon_1 - \frac{2}{3}\frac{y\varepsilon_1}{\alpha} + \varepsilon_4,\\
\Xi &= -\frac{1}{8}\frac{\lambda_2\left(27\alpha^4\lambda_2^2 - 36\alpha^2\varepsilon_1^2 + 48\beta\sigma - 48\beta - 16\sigma\right)t}{\alpha}\\
&\quad - \frac{3}{2}\alpha\lambda_2 x + \lambda_2 y + \lambda_4,\\
\Lambda &= -\frac{1}{12}\frac{t\int_1\left(81\alpha^4\lambda_2^2 - 12\alpha^2\varepsilon_1^2 + 48\beta\sigma - 48\beta - 16\sigma\right)}{\alpha^2}\\
&\quad - x\varepsilon_1 + \frac{2}{3}\frac{y\varepsilon_1}{\alpha} + \theta_4.
\end{aligned} \quad (54)$$

Case 14.

$$u_{CK} = -\frac{2}{\alpha}\frac{g_{CK}}{f_{CK}}\left(\frac{(\mathrm{d}f_{CK}/\mathrm{d}x)}{g_{CK}} - \frac{f_{CK}(\mathrm{d}g_{CK}/\mathrm{d}x)}{g_{CK}^2}\right), \quad (55)$$

in which,

$$
\begin{aligned}
f_{CK} &= e^{-\Omega} + \delta_4 e^{\Omega} - \delta_5 \sin(\Xi) + \delta_6 \sin h(\Lambda), g_{CK} \\
\Omega &= -\frac{t\left(\alpha^2\varepsilon_1^3 - 3\alpha^2\varepsilon_1\lambda_1^2 + 6\alpha\beta\sigma\varepsilon_2 - 2\alpha\sigma\varepsilon_2 + 4\beta\varepsilon_1\right)}{\alpha^2} + x\int_1 + y\int_2 + \int_4, \\
\Xi &= -\frac{1}{3}\frac{\omega t}{\alpha^2\delta_5^2\lambda_1} + \lambda_1 x - \frac{1}{3}\frac{y\left(3\alpha\delta_6^2\varepsilon_1\varepsilon_2 + 12\alpha\delta_4\varepsilon_1\varepsilon_2 + 2\delta_5^2\lambda_1^2 + 2\delta_6^2\varepsilon_1^2 + 8\delta_4\varepsilon_1^2\right)}{\alpha\delta_5^2\lambda_1} + \lambda_4, \\
\Lambda &= \frac{1}{3}\frac{\left(3\alpha^2\varepsilon_1^3 - 9\alpha^2\varepsilon_1\lambda_1^2 - 18\alpha\beta\sigma\varepsilon_2 + 6\alpha\sigma\varepsilon_2 - 24\beta\sigma\varepsilon_1 + 12\beta\varepsilon_1 + 8\sigma\varepsilon_1\right)t}{\alpha^2} - x\int_1 + \frac{1}{3}\frac{y(3\alpha\varepsilon_2 + 4\varepsilon_1)}{\alpha} + \theta_4, \\
\omega &= 9\alpha^2\delta_5^2\varepsilon_1^2\lambda_1^2 - 3\alpha^2\delta_5^2\lambda_1^4 - 18\alpha\beta\sigma\delta_6^2\varepsilon_1\varepsilon_2 - 72\alpha\beta\sigma\delta_4\varepsilon_1\varepsilon_2 + 6\alpha\sigma\delta_6^2\varepsilon_1\varepsilon_2 \\
&\quad - 12\beta\sigma\delta_5^2\lambda_1^2 - 12\beta\sigma\delta_6^2\varepsilon_1^2 + 24\alpha\sigma\delta_4\varepsilon_1\varepsilon_2 - 48\beta\sigma\delta_4\varepsilon_1^2 + 12\beta\delta_5^2\lambda_1^2 + 4\sigma\delta_5^2\lambda_1^2 + 4\sigma\delta_6^2\varepsilon_1^2 + 16\sigma\delta_4\varepsilon_1^2.
\end{aligned}
\tag{56}
$$

Figure 8 presents the overtaking interactions between two stripe waves and periodic wave containing 3D plot, density plot, and 2D plot, respectively, $(y = -1, 0, 1)$.

Case 15.

$$
u_{CK} = -\frac{2}{\alpha}\frac{g_{CK}}{f_{CK}}\left(\frac{\mathrm{d}f_{CK}/\mathrm{d}x}{g_{CK}} - \frac{f_{CK}\mathrm{d}g_{CK}/\mathrm{d}x}{g_{CK}^2}\right), \tag{57}
$$

in which,

$$
\begin{aligned}
f_{CK} &= e^{-\Omega} + \delta_4 e^{\Omega} + \delta_2 \sin(\Xi) + \delta_6 \sin h(\Lambda), g_{CK} \\
\Omega &= -\frac{1}{3}\frac{t\varepsilon_1\left(3\alpha^2\varepsilon_1^2 - 9\alpha^2\lambda_1^2 - 12\beta\sigma + 12\beta + 4\sigma\right)}{\alpha^2} + x\varepsilon_1 - \frac{2}{3}\frac{y\varepsilon_1}{\alpha} + \varepsilon_4, \\
\Xi &= -\frac{1}{3}\frac{\left(9\alpha^2\varepsilon_1^2 - 3\alpha^2\lambda_1^2 - 12\beta\sigma + 12\beta + 4\sigma\right)\lambda_1 t}{\alpha^2} + \lambda_1 x - \frac{2}{3}\frac{\lambda_1 y}{\alpha} + \lambda_4, \\
\Lambda &= \frac{1}{3}\frac{t\int_1\left(3\alpha^2\varepsilon_1^2 - 9\alpha^2\lambda_1^2 - 12\beta\sigma + 12\beta + 4\sigma\right)}{\alpha^2} - x\varepsilon_1 + \frac{2}{3}\frac{y\varepsilon_1}{\alpha} + \theta_4.
\end{aligned}
\tag{58}
$$

Figure 9 presents the overtaking interactions between two stripe waves and periodic wave containing 3D plot, density plot, and 2D plot, respectively, $(y = -1, 0, 1)$.

8. Periodic Wave Solutions

In the section, we will explore the periodic wave solutions for the $(2+1)$-dimensional Gardner equation. Let us consider a more general ansatz as follows:

$$
\begin{aligned}
f &= e^{-\varepsilon_1 x - \varepsilon_2 y - \varepsilon_3 t - \varepsilon_4} + \delta_1 e^{\varepsilon_1 x + \varepsilon_2 y + \varepsilon_3 t + \varepsilon_4} \\
&\quad + \delta_2 \cos(\lambda_1 x + \lambda_2 y + \lambda_3 t + \lambda_4) \\
&\quad + \delta_3 \cos h(2\lambda_1 x + 2\lambda_2 y + 2\lambda_3 t + 2\lambda_4),
\end{aligned}
\tag{59}
$$

$$
\begin{aligned}
g &= e^{-\varepsilon_1 x - \varepsilon_2 y - \varepsilon_3 t - \varepsilon_4} + \delta_4 e^{\varepsilon_1 x + \varepsilon_2 y + \varepsilon_3 t + \varepsilon_4} \\
&\quad + \delta_5 \cos(\lambda_1 x + \lambda_2 y + \lambda_3 t + \lambda_4) \\
&\quad + \delta_6 \cos h(2\lambda_1 x + 2\lambda_2 y + 2\lambda_3 t + 2\lambda_4).
\end{aligned}
\tag{60}
$$

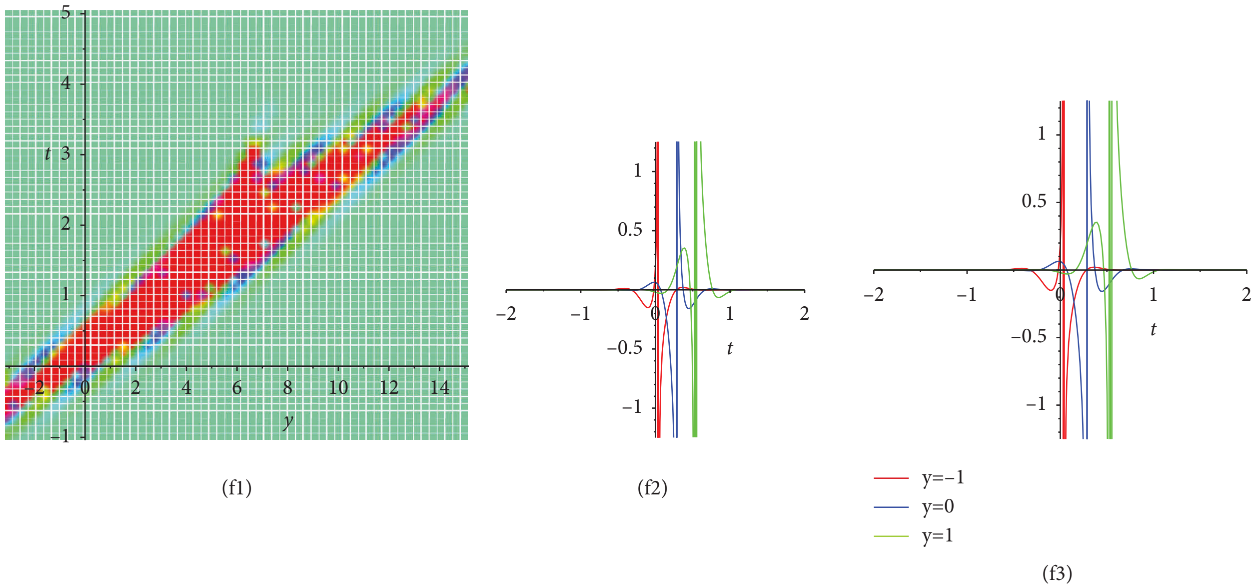

Figure 8: Behavior of cross-kink solution $u(x, y, t)$ in Eq. (70) with the selected amounts $\alpha = 1, \beta = 1, \sigma = 1, \int_1 = 1, \int_2 = 1.5, \int_4 = 2.5, \lambda_1 = 1$, $\lambda_4 = 1.2, \delta_4 = 2, \delta_5 = 3, \delta_6 = 2.5, \theta_2 = 1.5, \theta_4 = 2, x = 2$.

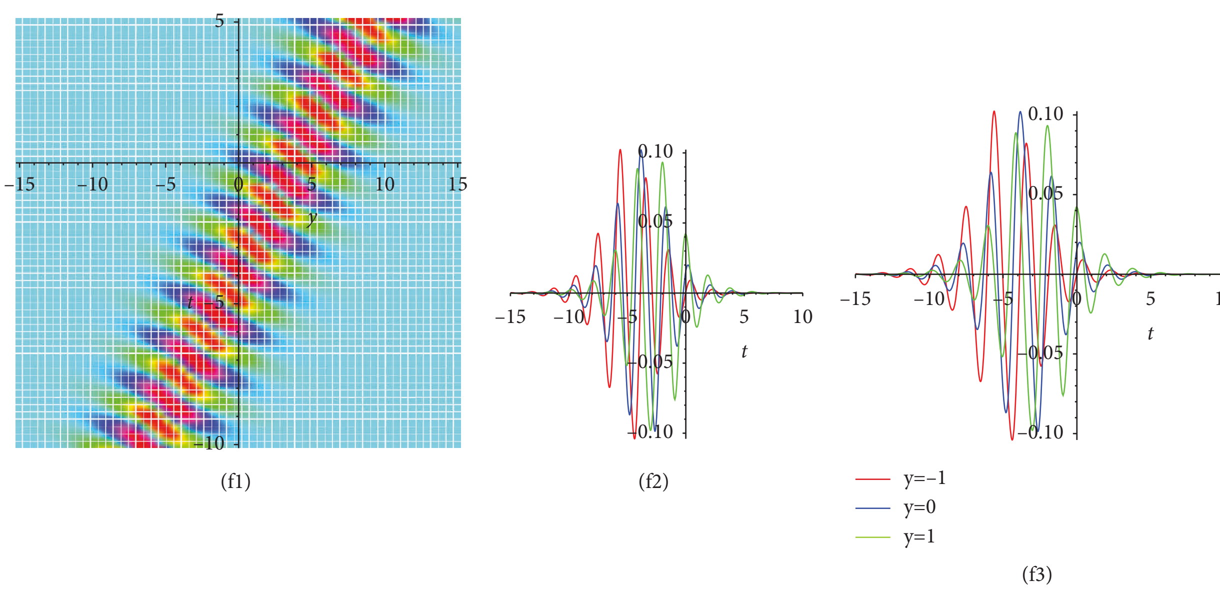

Figure 9: Behavior of cross-kink solution $u(x, y, t)$ in Eq. (73) with the selected amounts $\alpha = 1, \beta = 1, \sigma = 1, \epsilon_1 = 1, \epsilon_2 = 1.5, \epsilon_4 = 2.5, \lambda_1 = 1$, $\lambda_4 = 1.2, \delta_2 = 1.5, \delta_4 = 2, \delta_5 = 3, \delta_6 = 2.5, \theta_2 = 1.5, \theta_4 = 2, x = 2$.

Substituting (59) and (60) into Eq. (3) and collecting all relevant coefficients of exp, cos, sin, cos h, and sin h, a series of equations have been obtained. Solving these equations, we have the following cases:

Case 16.

$$\begin{aligned}
\int_{3} &= -\frac{\alpha^2\varepsilon_1^3 - 3\alpha^2\varepsilon_1\lambda_1^2 + 6\alpha\beta\sigma\varepsilon_2 - 2\alpha\sigma\varepsilon_2 + 4\beta\varepsilon_1}{\alpha^2}, \lambda_3\\
\lambda_2 &= -\frac{1}{3}\frac{3\alpha\delta_6^2\varepsilon_1\varepsilon_2 + 12\alpha\delta_4\varepsilon_1\varepsilon_2 + 2\delta_5^2\lambda_1^2 + 2\delta_6^2\varepsilon_1^2 + 8\delta_4\varepsilon_1^2}{\alpha\delta_5^2\lambda_1}, \theta_2\\
\omega &= 9\alpha^2\delta_5^2\varepsilon_1^2\lambda_1^2 - 3\alpha^2\delta_5^2\lambda_1^4 - 18\alpha\beta\sigma\delta_6^2\varepsilon_1\varepsilon_2 - 72\alpha\beta\sigma\delta_4\varepsilon_1\varepsilon_2 + 6\alpha\sigma\delta_6^2\varepsilon_1\varepsilon_2 - 12\beta\sigma\delta_5^2\lambda_1^2\\
&\quad - 12\beta\sigma\delta_6^2\varepsilon_1^2 + 24\alpha\sigma\delta_4\varepsilon_1\varepsilon_2 - 48\beta\sigma\delta_4\varepsilon_1^2 + 12\beta\delta_5^2\lambda_1^2 + 4\sigma\delta_5^2\lambda_1^2 + 4\sigma\delta_6^2\varepsilon_1^2 + 16\sigma\delta_4\varepsilon_1^2,\\
\theta_3 &= -\frac{1}{3}\frac{3\alpha^2\varepsilon_1^3 - 9\alpha^2\varepsilon_1\lambda_1^2 - 18\alpha\beta\sigma\varepsilon_2 + 6\alpha\sigma\varepsilon_2 - 24\beta\sigma\varepsilon_1 + 12\beta\varepsilon_1 + 8\sigma\varepsilon_1}{\alpha^2}.
\end{aligned} \tag{61}$$

Under the transformation $u = -2/\alpha(\ln g/f)_x$, the corresponding special periodic wave solution is read as follows:

$$u_{CK} = -\frac{2}{\alpha}\frac{g_{CK}}{f_{CK}}\left(\frac{\mathrm{d}f_{CK}/\mathrm{d}x}{g_{CK}} - \frac{f_{CK}\mathrm{d}g_{CK}/\mathrm{d}x}{g_{CK}^2}\right), \tag{62}$$

in which,

$$\begin{aligned}
f_{CK} &= e^{-\Omega} + \delta_4 e^{\Omega} - \delta_5\sin(\Xi) + \delta_3\sin h(\Lambda),\\
g_{CK} &= e^{-\Omega} + \delta_4 e^{\Omega} + \delta_5\sin(\Xi) + \delta_3\sin h(\Lambda),\\
\Omega &= -\frac{t\left(\alpha^2\varepsilon_1^3 - 3\alpha^2\varepsilon_1\lambda_1^2 + 6\alpha\beta\sigma\varepsilon_2 - 2\alpha\sigma\varepsilon_2 + 4\beta\varepsilon_1\right)}{\alpha^2} + x\varepsilon_1 + y\varepsilon_2 + \varepsilon_4,\\
\Xi &= -\frac{1}{3}\frac{\omega t}{\alpha^2\delta_5^2\lambda_1} + \lambda_1 x - \frac{1}{3}\frac{y\left(-3\alpha\delta_6^2\varepsilon_1\varepsilon_2 + 12\alpha\delta_4\varepsilon_1\varepsilon_2 + 2\delta_5^2\lambda_1^2 - 2\delta_6^2\varepsilon_1^2 + 8\delta_4\varepsilon_1^2\right)}{\alpha\delta_5^2\lambda_1} + \lambda_4,\\
\Lambda &= -\frac{1}{3}\frac{\left(3\alpha^2\varepsilon_1^3 - 9\alpha^2\varepsilon_1\lambda_1^2 - 18\alpha\beta\sigma\varepsilon_2 + 6\alpha\sigma\varepsilon_2 - 24\beta\sigma\varepsilon_1 + 12\beta\varepsilon_1 + 8\sigma\varepsilon_1\right)t}{\alpha^2} + x\varepsilon_1 - \frac{1}{3}\frac{\left(3\alpha\varepsilon_2 + 4\varepsilon_1\right)y}{\alpha} + \theta_4.
\end{aligned} \tag{63}$$

Case 17.

$$u_{CK} = -\frac{2}{\alpha}\frac{g_{CK}}{f_{CK}}\left(\frac{\mathrm{d}f_{CK}/\mathrm{d}x}{g_{CK}} - \frac{f_{CK}\mathrm{d}g_{CK}/\mathrm{d}x}{g_{CK}^2}\right), \tag{64}$$

in which,

$$\begin{aligned}
f_{CK} &= e^{-\Omega} + \frac{1}{4}\delta_6^2 e^{\Omega} - \delta_5\cos(\Xi) + \delta_6\cos h(\Lambda),\\
g_{CK} &= e^{-\Omega} + \frac{1}{4}\delta_6^2 e^{\Omega} + \delta_5\cos(\Xi) + \delta_6\cos h(\Lambda),\\
\Omega &= -\frac{t\left(\alpha^2\varepsilon_1^3 + 6\alpha\beta\sigma\varepsilon_2 - 2\alpha\sigma\varepsilon_2 + 4\beta\varepsilon_1\right)}{\alpha^2} + x\varepsilon_1 + y\varepsilon_2 + \varepsilon_4, \Xi\\
\Lambda &= -\frac{1}{3}\frac{\left(3\alpha^2\varepsilon_1^3 - 18\alpha\beta\sigma\varepsilon_2 + 6\alpha\sigma\varepsilon_2 - 24\beta\sigma\varepsilon_1 + 12\beta\varepsilon_1 + 8\sigma\varepsilon_1\right)t}{\alpha^2} + x\varepsilon_1 - \frac{1}{3}\frac{y\left(3\alpha\varepsilon_2 + 4\varepsilon_1\right)}{\alpha} + \theta_4.
\end{aligned} \tag{65}$$

Case 18.

$$u_{CK} = -\frac{2}{\alpha}\frac{g_{CK}}{f_{CK}}\left(\frac{\mathrm{d}f_{CK}/\mathrm{d}x}{g_{CK}} - \frac{f_{CK}\mathrm{d}g_{CK}/\mathrm{d}x}{g_{CK}^2}\right), \tag{66}$$

in which,

$$\begin{aligned}
f_{CK} &= e^{-\Omega} + \delta_4 e^{\Omega} - \delta_5\cos(\Xi) + \delta_6\cos h(\Lambda),\\
g_{CK} &= e^{-\Omega} + \delta_4 e^{\Omega} + \delta_5\cos(\Xi) + \delta_6\cos h(\Lambda),\\
\Omega &= -\frac{1}{3}\frac{t\int_1\left(3\alpha^2\varepsilon_1^2 - 12\beta\sigma + 12\beta + 4\sigma\right)}{\alpha^2}\\
&\quad + x\varepsilon_1 - \frac{2}{3}\frac{y\varepsilon_1}{\alpha} + \varepsilon_4,\\
\Xi &= -2\frac{\sigma\lambda_2(3\beta - 1)t}{\alpha} + \lambda_2 y + \lambda_4,\\
\Lambda &= -\frac{1}{3}\frac{t\int_1\left(3\alpha^2\varepsilon_1^2 - 12\beta\sigma + 12\beta + 4\sigma\right)}{\alpha^2}\\
&\quad + x\varepsilon_1 - \frac{2}{3}\frac{y\varepsilon_1}{\alpha} + \theta_4.
\end{aligned} \tag{67}$$

Case 19.

$$u_{CK} = -\frac{2}{\alpha}\frac{g_{CK}}{f_{CK}}\left(\frac{\mathrm{d}f_{CK}/\mathrm{d}x}{g_{CK}} - \frac{f_{CK}\mathrm{d}g_{CK}/\mathrm{d}x}{g_{CK}^2}\right), \tag{68}$$

in which,

$$\begin{aligned}
f_{CK} &= e^{-\Omega} + \delta_4 e^{\Omega} + \delta_2\cos(\Xi) + \delta_6\cos h(\Lambda),\\
g_{CK} &= e^{-\Omega} + \delta_4 e^{\Omega} + \delta_5\cos(\Xi) + \delta_6\cos h(\Lambda),\\
\Omega &= -\frac{1}{3}\frac{t\varepsilon_1\left(3\alpha^2\varepsilon_1^2 - 9\alpha^2\lambda_1^2 - 12\beta\sigma + 12\beta + 4\sigma\right)}{\alpha^2}\\
&\quad + x\varepsilon_1 - \frac{2}{3}\frac{y\varepsilon_1}{\alpha} + \varepsilon_4,\\
\Xi &= -\frac{1}{3}\frac{\left(9\alpha^2\varepsilon_1^2 - 3\alpha^2\lambda_1^2 - 12\beta\sigma + 12\beta + 4\sigma\right)\lambda_1 t}{\alpha^2}\\
&\quad + \lambda_1 x - \frac{2}{3}\frac{y\lambda_1}{\alpha} + \lambda_4,\\
\Lambda &= -\frac{1}{3}\frac{t\int_1\left(3\alpha^2\varepsilon_1^2 - 9\alpha^2\lambda_1^2 - 12\beta\sigma + 12\beta + 4\sigma\right)}{\alpha^2}\\
&\quad + x\varepsilon_1 - \frac{2}{3}\frac{y\varepsilon_1}{\alpha} + \theta_4.
\end{aligned} \tag{69}$$

Case 20.

$$u_{CK} = -\frac{2}{\alpha}\frac{g_{CK}}{f_{CK}}\left(\frac{\mathrm{d}f_{CK}/\mathrm{d}x}{g_{CK}} - \frac{f_{CK}\mathrm{d}g_{CK}/\mathrm{d}x}{g_{CK}^2}\right), \tag{70}$$

in which,

$$
\begin{aligned}
f_{CK} &= e^{-\Omega} + \delta_2 \cos(\Xi) + \delta_6 \cos h(\Lambda),\\
g_{CK} &= e^{-\Omega} + \delta_5 \cos(\Xi) + \delta_6 \cos h(\Lambda),\\
\Omega &= \frac{1}{12}\frac{t\varepsilon_1\left(81\alpha^4\lambda_2^2 - 12\alpha^2\varepsilon_1^2 + 48\beta\sigma - 48\beta - 16\sigma\right)}{\alpha^2}\\
&\quad + x\varepsilon_1 - \frac{2}{3}\frac{y\varepsilon_1}{\alpha} + \varepsilon_4,\\
\Xi &= -\frac{1}{8}\frac{\lambda_2\left(27\alpha^4\lambda_2^2 - 36\alpha^2\varepsilon_1^2 + 48\beta\sigma - 48\beta - 16\sigma\right)t}{\alpha}\\
&\quad - \frac{3}{2}\alpha\lambda_2 x + \lambda_2 y + \lambda_4,\\
\Lambda &= -\frac{1}{12}\frac{t\int_1\left(81\alpha^4\lambda_2^2 - 12\alpha^2\varepsilon_1^2 + 48\beta\sigma - 48\beta - 16\sigma\right)}{\alpha^2}\\
&\quad - x\varepsilon_1 + \frac{2}{3}\frac{y\varepsilon_1}{\alpha} + \theta_4.
\end{aligned}
\tag{71}
$$

Case 21.

$$
u_{CK} = -\frac{2}{\alpha}\frac{g_{CK}}{f_{CK}}\left(\frac{\mathrm{d}f_{CK}/\mathrm{d}x}{g_{CK}} - \frac{f_{CK}\mathrm{d}g_{CK}/\mathrm{d}x}{g_{CK}^2}\right), \tag{72}
$$

in which,

$$
\begin{aligned}
f_{CK} &= e^{-\Omega} + \delta_4 e^{\Omega} - \delta_5 \cos(\Xi) + \delta_6 \cos h(\Lambda),\\
g_{CK} &= e^{-\Omega} + \delta_4 e^{\Omega} + \delta_5 \cos(\Xi) + \delta_6 \cos h(\Lambda),\\
\Omega &= -\frac{t\left(\alpha^2\varepsilon_1^3 - 3\alpha^2\varepsilon_1\lambda_1^2 + 6\alpha\beta\sigma\varepsilon_2 - 2\alpha\sigma\varepsilon_2 + 4\beta\varepsilon_1\right)}{\alpha^2} + x\varepsilon_1 + y\varepsilon_2 + \varepsilon_4,\\
\Xi &= -\frac{1}{3}\frac{\omega t}{\alpha^2\delta_5^2\lambda_1} + \lambda_1 x - \frac{1}{3}\frac{y\left(3\alpha\delta_6^2\varepsilon_1\varepsilon_2 + 12\alpha\delta_4\varepsilon_1\varepsilon_2 + 2\delta_5^2\lambda_1^2 + 2\delta_6^2\varepsilon_1^2 + 8\delta_4\varepsilon_1^2\right)}{\alpha\delta_5^2\lambda_1} + \lambda_4,\\
\Lambda &= \frac{1}{3}\frac{\left(3\alpha^2\varepsilon_1^3 - 9\alpha^2\varepsilon_1\lambda_1^2 - 18\alpha\beta\sigma\varepsilon_2 + 6\alpha\sigma\varepsilon_2 - 24\beta\sigma\varepsilon_1 + 12\beta\varepsilon_1 + 8\sigma\varepsilon_1\right)t}{\alpha^2} - x\varepsilon_1 + \frac{1}{3}\frac{y\left(3\alpha\varepsilon_2 + 4\varepsilon_1\right)}{\alpha} + \theta_4,\\
\omega &= 9\alpha^2\delta_5^2\varepsilon_1^2\lambda_1^2 - 3\alpha^2\delta_5^2\lambda_1^4 - 18\alpha\beta\sigma\delta_6^2\varepsilon_1\varepsilon_2 - 72\alpha\beta\sigma\delta_4\varepsilon_1\varepsilon_2 + 6\alpha\sigma\delta_6^2\varepsilon_1\varepsilon_2\\
&\quad - 12\beta\sigma\delta_5^2\lambda_1^2 - 12\beta\sigma\delta_6^2\varepsilon_1^2 + 24\alpha\sigma\delta_4\varepsilon_1\varepsilon_2 - 48\beta\sigma\delta_4\varepsilon_1^2 + 12\beta\delta_5^2\lambda_1^2 + 4\sigma\delta_5^2\lambda_1^2 + 4\sigma\delta_6^2\varepsilon_1^2 + 16\sigma\delta_4\varepsilon_1^2.
\end{aligned}
\tag{73}
$$

Figure 10 presents the overtaking interactions between two stripe waves and periodic wave containing 3D plot, density plot, and 2D plot, respectively, $(t = 1, 2, 3)$.

Case 22.

$$
u_{CK} = -\frac{2}{\alpha}\frac{g_{CK}}{f_{CK}}\left(\frac{\mathrm{d}f_{CK}/\mathrm{d}x}{g_{CK}} - \frac{f_{CK}\mathrm{d}g_{CK}/\mathrm{d}x}{g_{CK}^2}\right), \tag{74}
$$

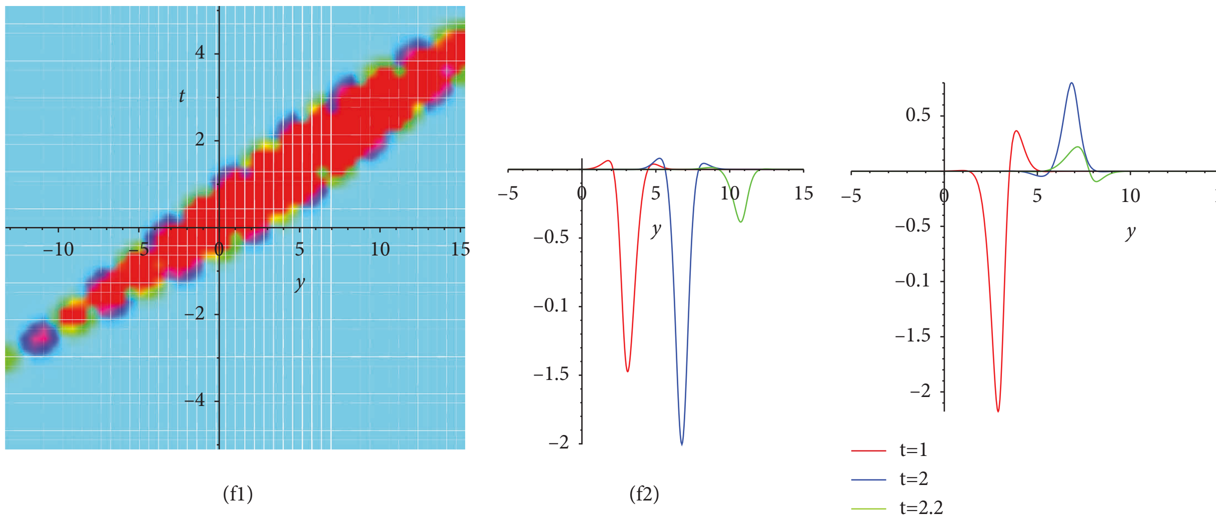

(f1) (f2) (f3)

Figure 10: Behavior of periodic wave solution $u(x,y,t)$ in Eq. (72) with the selected amounts $\alpha = 1, \beta = 1, \sigma = 1, \int_1 = 1, \int_2 = 1.5, \int_4 = 2.5, \lambda_1 = 1, \lambda_4 = 1.2, \delta_4 = 2, \delta_5 = 3, \delta_6 = 2.5, \theta_2 = 1.5, \theta_4 = 2, x = 2$.

in which,

$$\begin{aligned}
f_{CK} &= e^{-\Omega} + \delta_4 e^{\Omega} + \delta_2 \cos(\Xi) + \delta_6 \cos h(\Lambda),\\
g_{CK} &= e^{-\Omega} + \delta_4 e^{\Omega} + \delta_5 \cos(\Xi) + \delta_6 \cos h(\Lambda),\\
\Omega &= -\frac{1}{3}\frac{t\varepsilon_1\left(3\alpha^2\varepsilon_1^2 - 9\alpha^2\lambda_1^2 - 12\beta\sigma + 12\beta + 4\sigma\right)}{\alpha^2}\\
&\quad + x\varepsilon_1 - \frac{2}{3}\frac{y\varepsilon_1}{\alpha} + \varepsilon_4,\\
\Xi &= -\frac{1}{3}\frac{\left(9\alpha^2\varepsilon_1^2 - 3\alpha^2\lambda_1^2 - 12\beta\sigma + 12\beta + 4\sigma\right)\lambda_1 t}{\alpha^2}\\
&\quad + \lambda_1 x - \frac{2}{3}\frac{\lambda_1 y}{\alpha} + \lambda_4,\\
\Lambda &= \frac{1}{3}\frac{t\varepsilon_1\left(3\alpha^2\varepsilon_1^2 - 9\alpha^2\lambda_1^2 - 12\beta\sigma + 12\beta + 4\sigma\right)}{\alpha^2}\\
&\quad - x\varepsilon_1 + \frac{2}{3}\frac{y\varepsilon_1}{\alpha} + \theta_4.
\end{aligned} \tag{75}$$

Figure 11 presents the overtaking interactions between two stripe waves and periodic wave containing 3D plot, density plot, and 2D plot, respectively, $(y = -1, 0, 1)$.

9. Multiwave Solutions

In the section, we will explore the multiwave solutions for the $(2+1)$-dimensional Gardner equation. Let us consider a more general ansatz as follows:

$$\begin{aligned}
f &= \delta_1 \cos h(\varepsilon_1 x + \varepsilon_2 y + \varepsilon_3 t + \varepsilon_4)\\
&\quad + \delta_2 \cos(\lambda_1 x + \lambda_2 y + \lambda_3 t + \lambda_4)\\
&\quad + \delta_3 \cos h(2\lambda_1 x + 2\lambda_2 y + 2\lambda_3 t + 2\lambda_4),
\end{aligned} \tag{76}$$

$$\begin{aligned}
g &= \delta_4 \cos h(\varepsilon_1 x + \varepsilon_2 y + \varepsilon_3 t + \varepsilon_4)\\
&\quad + \delta_5 \cos(\lambda_1 x + \lambda_2 y + \lambda_3 t + \lambda_4)\\
&\quad + \delta_6 \cos h(2\lambda_1 x + 2\lambda_2 y + 2\lambda_3 t + 2\lambda_4).
\end{aligned} \tag{77}$$

Substituting (76) and (77) into Eq. (3) and collecting all relevant coefficients of exp, cos, sin, cos h, and sin h, a series of equations have been obtained. Solving these equations, we have the following cases:

Case 23.

$$\begin{aligned}
\delta_2 &= \frac{\delta_1\delta_5}{\delta_4}, \delta_3 = \frac{\delta_1\delta_6}{\delta_4}, \varepsilon_2 = -\frac{2}{3}\frac{\varepsilon_1}{\alpha},\\
\varepsilon_3 &= -\frac{1}{3}\frac{\varepsilon_1\left(3\alpha^2\varepsilon_1^2 - 12\beta\sigma + 12\beta + 4\sigma\right)}{\alpha^2}, \lambda_1 = -\frac{3}{2}\alpha\lambda_2.
\end{aligned} \tag{78}$$

Under the transformation $u = -2/\alpha(\ln g/f)_x$, the corresponding special multiwave solution is read as follows:

$$u_{CK} = -\frac{2}{\alpha}\frac{g_{CK}}{f_{CK}}\left(\frac{\mathrm{d}f_{CK}/\mathrm{d}x}{g_{CK}} - \frac{f_{CK}\mathrm{d}g_{CK}/\mathrm{d}x}{g_{CK}^2}\right), \tag{79}$$

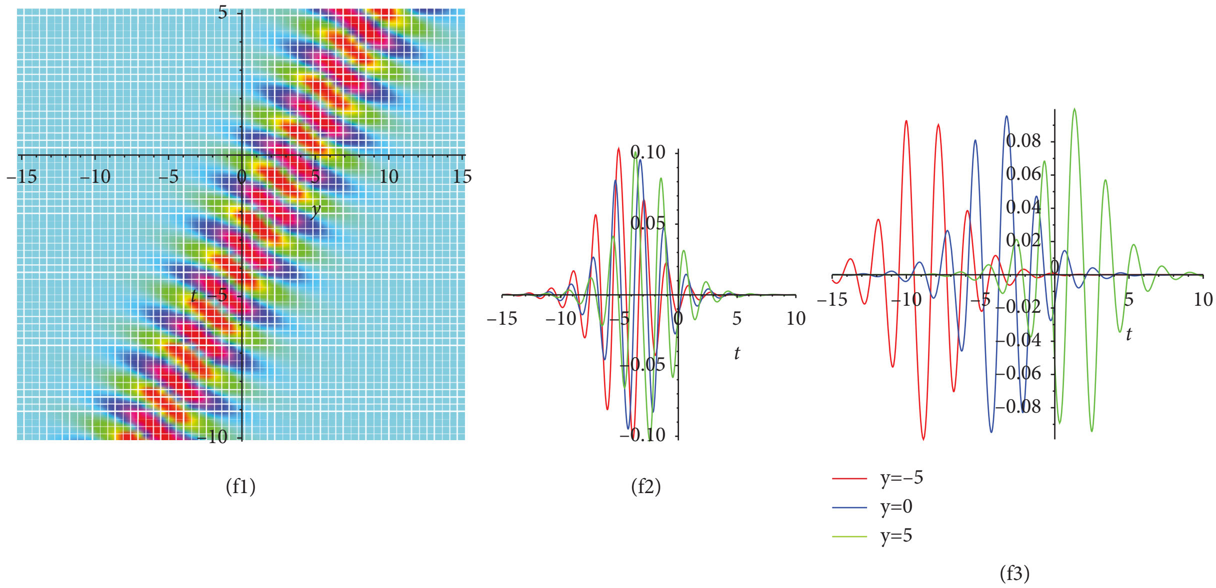

Figure 11: Behavior of periodic wave solution $u(x, y, t)$ in Eq. (74) with the selected amounts $\alpha = 1, \beta = 1, \sigma = 1, \int_1 = 1, \int_2 = 1.5, \int_4 = 2.5, \lambda_1 = 1, \lambda_4 = 1.2, \delta_2 = 1.5, \delta_4 = 2, \delta_5 = 3, \delta_6 = 2.5, \theta_2 = 1.5, \theta_4 = 2, x = 2$.

in which,

$$\begin{aligned} f_{CK} &= \delta_1 \cos h(\Omega) + \frac{\delta_1\delta_5}{\delta_4}\cos(\Xi) + \frac{\delta_1\delta_6}{\delta_4}\cos h(\Lambda), \\ g_{CK} &= \delta_4 \cos h(\Omega) + \delta_5 \cos(\Xi) + \delta_6 \cos h(\Lambda), \\ \Omega &= -\frac{1}{3}\frac{t\int_1\left(3\alpha^2\varepsilon_1^2 - 12\beta\sigma + 12\beta + 4\sigma\right)}{\alpha^2} \\ &\quad + x\varepsilon_1 - \frac{2}{3}\frac{y\varepsilon_1}{\alpha} + \varepsilon_4, \\ \Xi &= \lambda_3 t - \frac{3}{2}\alpha\lambda_2 x + \lambda_2 y + \lambda_4, \Lambda = t\theta_3 + \theta_4. \end{aligned} \tag{80}$$

Figure 12 presents the overtaking interactions between two stripe waves and periodic wave containing 3D plot, contour plot, and 2D plot, respectively, $(t = -0.5, 0, 0.5)$.

Case 24.

$$\begin{aligned} \delta_2 &= \frac{\delta_1\delta_5}{\delta_4}, \delta_3 = \frac{\delta_1\delta_6}{\delta_4}, \varepsilon_2 = -\frac{2}{3}\frac{\varepsilon_1}{\alpha}, \\ \varepsilon_3 &= -\frac{1}{12}\frac{\int_1\left(81\alpha^4\theta_2^2 + 12\alpha^2\varepsilon_1^2 - 48\beta\sigma + 48\beta + 16\sigma\right)}{\alpha^2}, \\ \theta_1 &= -\frac{3}{2}\alpha\theta_2. \end{aligned} \tag{81}$$

Under the transformation $u = -2/\alpha(\ln g/f)_x$, the corresponding special multiwave solution is read as follows:

$$u_{CK} = -\frac{2}{\alpha}\frac{g_{CK}}{f_{CK}}\left(\frac{\mathrm{d}f_{CK}/\mathrm{d}x}{g_{CK}} - \frac{f_{CK}\mathrm{d}g_{CK}/\mathrm{d}x}{g_{CK}^2}\right), \tag{82}$$

in which,

$$\begin{aligned} f_{CK} &= \delta_1 \cos h(\Omega) + \frac{\delta_1\delta_5}{\delta_4}\cos(\Xi) + \frac{\delta_1\delta_6}{\delta_4}\cos h(\Lambda), \\ g_{CK} &= \delta_4 \cos h(\Omega) + \delta_5 \cos(\Xi) + \delta_6 \cos h(\Lambda), \\ \Omega &= -\frac{1}{12}\frac{t\epsilon_1\left(81\alpha^4\theta_2^2 + 12\alpha^2\epsilon_1^2 - 48\beta\sigma + 48\beta + 16\sigma\right)}{\alpha^2} \\ &\quad + x\epsilon_1 - \frac{2}{3}\frac{y\epsilon_1}{\alpha} + \epsilon_4, \\ \Xi &= t\lambda_3 + \lambda_4, \Lambda = \theta_3 t - \frac{3}{2}\alpha\theta_2 x + \theta_2 y + \theta_4. \end{aligned} \tag{83}$$

Figure 13 presents the overtaking interactions between two stripe waves and periodic wave containing density plot and 2D plot, respectively, $(t = 0.0, 0.01, 0.1)$.

9.1. Solitary Wave Solutions. Here, we will consider the solitary wave solution by selecting the below function in which (1) has been taken as follows:

$$\begin{aligned} f &= \delta_1 \exp\left(\varepsilon_1 x + \varepsilon_2 y + \varepsilon_3 t + \varepsilon_4\right) \\ &\quad + \delta_2 \exp\left(\lambda_1 x + \lambda_2 y + \lambda_3 t + \lambda_4\right) + \delta_3, \end{aligned} \tag{84}$$

$$\begin{aligned} g &= \delta_4 \exp\left(\varepsilon_1 x + \varepsilon_2 y + \varepsilon_3 t + \varepsilon_4\right) \\ &\quad + \delta_5 \exp\left(\lambda_1 x + \lambda_2 y + \lambda_3 t + \lambda_4\right) + \delta_6. \end{aligned} \tag{85}$$

Plugging (84) and (85) into Eq. (3) and collecting all relevant coefficients of $\exp\Omega$ and $\exp\Xi$, a series of equations have been obtained. Solving these equations, we have the following solutions:

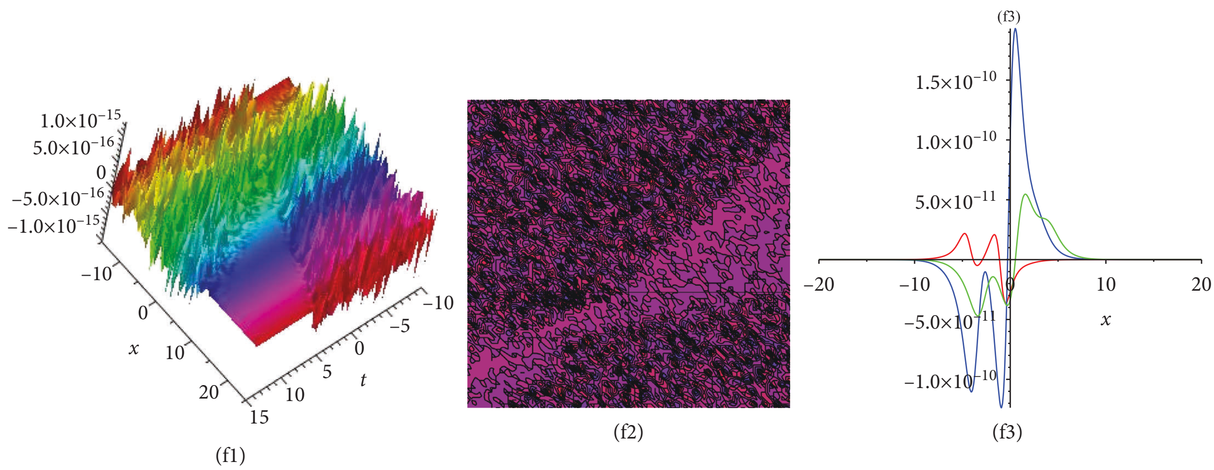

Figure 12: Behavior of multiwave solution $u(x, y, t)$ in Eq. (78) with the selected amounts $\alpha = 1, \beta = 1, \sigma = 1, \int_1 = 1, \int_4 = 2.5, \lambda_2 = 1, \lambda_3 = 2, \lambda_4 = 1.2, \delta_1 = 2.3, \delta_4 = 2, \delta_5 = 3, \delta_6 = 2.5, \theta_3 = 1.5, \theta_4 = 2, y = 2$.

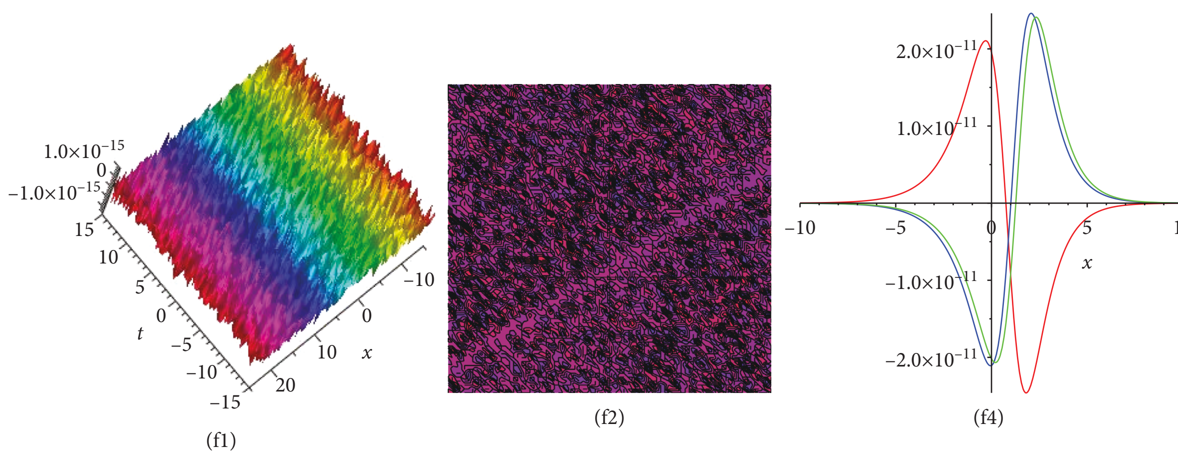

Figure 13: Behavior of multiwave solution $u(x, y, t)$ in Eq. (79) with the selected amounts $\alpha = 1, \beta = 1, \sigma = 1, \int_1 = 1, \int_4 = 2.5, \lambda_3 = .5, \lambda_4 = 1, \delta_1 = 2.3, \delta_4 = 2, \delta_5 = 3, \delta_6 = 2.5, \theta_2 = .5, \theta_3 = .5, \theta_4 = 2, y = 2$.

9.1.1. First Solution. Under the transformation $u = -2/\alpha (\ln g/f)_x$, the corresponding special solitary wave solution is read as follows:

$$u_S = -\frac{2}{\alpha}\frac{g_S}{f_S}\left(\frac{\mathrm{d}f_S/\mathrm{d}x}{g_S} - \frac{f_S \mathrm{d}g_S/\mathrm{d}x}{g_S^2}\right), \tag{86}$$

in which,

$$\begin{aligned}
&f_S = \delta_1 \exp(\Omega) + \delta_2 \exp(\Xi) + \delta_3, g_S = \delta_4 \exp(\Omega) + \delta_5 \exp(\Xi) + \frac{\delta_3\delta_4\left(2\delta_1\delta_5\int_1 + \delta_1\delta_5\lambda_1 + \delta_2\delta_4\lambda_1\right)}{\delta_1\left(\delta_1\delta_5\lambda_1 + 2\delta_2\delta_4\int_1 + \delta_2\delta_4\lambda_1\right)},\\
&\Omega = -\frac{t\omega_1}{(\delta_1\delta_5 - \delta_2\delta_4)\alpha^2} + x\epsilon_1 + y\epsilon_2 + \epsilon_4,\\
&\Xi = -\frac{1}{3}\frac{\omega_2\lambda_1 t}{(\delta_1\delta_5 - \delta_2\delta_4)^2\alpha^2} - \lambda_1 x - \frac{1}{3}\frac{\lambda_1\left(3\alpha\delta_1\delta_5\int_1 + 3\alpha\delta_1\delta_5\lambda_1 + 3\alpha\delta_2\delta_4\int_1 + 3\alpha\delta_2\delta_4\lambda_1 - 2\delta_1\delta_5 + 2\delta_2\delta_4\right)y}{\alpha(\delta_1\delta_5 - \delta_2\delta_4)} - \lambda_4,\\
&\omega_1 = \alpha^2\delta_1\delta_5\varepsilon_1^3 - \alpha^2\delta_2\delta_4\varepsilon_1^3 - 3\alpha^2\delta_1\delta_5\varepsilon_1\varepsilon_2 - 3\alpha^2\delta_1\delta_5\varepsilon_2\lambda_1 - 3\alpha^2\delta_2\delta_4\varepsilon_1\varepsilon_2 - 3\alpha^2\delta_2\delta_4\varepsilon_2\lambda_1 + 6\alpha\beta\sigma\delta_1\delta_5\varepsilon_2\\
&\quad - 6\alpha\beta\sigma\delta_2\delta_4\varepsilon_2 - 2\alpha\sigma\delta_1\delta_5\varepsilon_2 + 2\alpha\sigma\delta_2\delta_4\varepsilon_2 - 2\alpha\delta_1\delta_5\varepsilon_1^2 - 2\alpha\delta_1\delta_5\varepsilon_1\lambda_1 - 2\alpha\delta_2\delta_4\varepsilon_1^2 - 2\alpha\delta_2\delta_4\varepsilon_1\lambda_1 + 4\beta\delta_1\delta_5\varepsilon_1 - 4\beta\delta_2\delta_4\varepsilon_1,\\
&\omega_2 = 9\alpha^2\delta_1^2\delta_5^2\varepsilon_1\lambda_1 + 6\alpha^2\delta_1^2\delta_5^2\lambda_1^2 + 36\alpha^2\delta_1\delta_2\delta_4\delta_5\varepsilon_1^2 + 54\alpha^2\delta_1\delta_2\delta_4\delta_5\varepsilon_1\lambda_1 + 24\alpha^2\delta_1\delta_2\delta_4\delta_5\lambda_1^2 + 9\alpha^2\delta_2^2\delta_4^2\varepsilon_1\lambda_1 + 6\alpha^2\delta_2^2\delta_4^2\lambda_1^2\\
&\quad - 18\alpha\beta\sigma\delta_1^2\delta_5^2\varepsilon_1 - 18\alpha\beta\sigma\delta_1^2\delta_5^2\lambda_1 + 18\alpha\beta\sigma\delta_2^2\delta_4^2\varepsilon_1 + 18\alpha\beta\sigma\delta_2^2\delta_4^2\lambda_1 + 6\alpha\sigma\delta_1^2\delta_5^2\varepsilon_1 + 6\alpha\sigma\delta_1^2\delta_5^2\lambda_1 - 6\alpha\sigma\delta_2^2\delta_4^2\varepsilon_1 - 6\alpha\sigma\delta_2^2\delta_4^2\lambda_1\\
&\quad + 12\beta\sigma\delta_1^2\delta_5^2 - 24\beta\sigma\delta_1\delta_2\delta_4\delta_5 + 12\beta\sigma\delta_2^2\delta_4^2 - 12\beta\delta_1^2\delta_5^2 + 24\beta\delta_1\delta_2\delta_4\delta_5 - 12\beta\delta_2^2\delta_4^2 - 4\sigma\delta_1^2\delta_5^2 + 8\sigma\delta_1\delta_2\delta_4\delta_5 - 4\sigma\delta_2^2\delta_4^2.
\end{aligned} \tag{87}$$

9.1.2. Second Solution. Under the transformation $u = -2/\alpha (\ln g/f)_x$, the corresponding special solitary wave solution is read as follows:

$$u_S = -\frac{2}{\alpha}\frac{g_S}{f_S}\left(\frac{\mathrm{d}f_S/\mathrm{d}x}{g_S} - \frac{f_S \mathrm{d}g_S/\mathrm{d}x}{g_S^2}\right), \tag{88}$$

in which,

$$\begin{aligned}
&f_S = \delta_1 \exp(\Omega) + \frac{\delta_1\delta_5}{\delta_4}\exp(\Xi) + \delta_3, g_S = \delta_4 \exp(\Omega) + \delta_5 \exp(\Xi) + \delta_6,\\
&\Omega = -\frac{t\omega_1}{\alpha^2(\delta_1\delta_6 - \delta_3\delta_4)} + x\varepsilon_1 + y\varepsilon_2 + \varepsilon_4, \Xi = -\frac{\omega_2 t}{\alpha^2(\delta_1\delta_6 - \delta_3\delta_4)} + x\varepsilon_1 - \lambda_2 y - \lambda_4,\\
&\omega_1 = \alpha^2\delta_1\delta_6\varepsilon_1^3 - \alpha^2\delta_3\delta_4\varepsilon_1^3 - 3\alpha^2\delta_1\delta_6\varepsilon_1\varepsilon_2 - 3\alpha^2\delta_3\delta_4\varepsilon_1\varepsilon_2 + 6\alpha\beta\sigma\delta_1\delta_6\varepsilon_2 - 6\alpha\beta\sigma\delta_3\delta_4\varepsilon_2\\
&\quad - 2\alpha\sigma\delta_1\delta_6\varepsilon_2 + 2\alpha\sigma\delta_3\delta_4\varepsilon_2 - 2\alpha\delta_1\delta_6\varepsilon_1^2 - 2\alpha\delta_3\delta_4\varepsilon_1^2 + 4\beta\delta_1\delta_6\varepsilon_1 - 4\beta\delta_3\delta_4\varepsilon_1,\\
&\omega_2 = \alpha^2\delta_1\delta_6\varepsilon_1^3 - \alpha^2\delta_3\delta_4\varepsilon_1^3 + 3\alpha^2\delta_1\delta_6\varepsilon_1\lambda_2 + 3\alpha^2\delta_3\delta_4\varepsilon_1\lambda_2 - 6\alpha\beta\sigma\delta_1\delta_6\lambda_2 + 6\alpha\beta\sigma\delta_3\delta_4\lambda_2\\
&\quad + 2\alpha\sigma\delta_1\delta_6\lambda_2 - 2\alpha\sigma\delta_3\delta_4\lambda_2 - 2\alpha\delta_1\delta_6\varepsilon_1^2 - 2\alpha\delta_3\delta_4\varepsilon_1^2 + 4\beta\delta_1\delta_6\varepsilon_1 - 4\beta\delta_3\delta_4\varepsilon_1.
\end{aligned} \tag{89}$$

10. Conclusion

In this paper, the lump solutions, lumpoff solutions, and rogue waves with predictability of the $(2+1)$-dimensional Gardner equation are investigated with more arbitrary autocephalous parameters. It is not hard to see that the general lump solution is an algebraically localized wave decayed in all space directions and exists in all time. We constructed a general quadratic function because of deriving the general lump solution for this equation. Hence, the lumpoff solutions are shown with more free autocephalous parameters, in which the lump solution localized in all directions in space. Moreover, when the lump solution is cut by twin-solitons, the special rogue waves are also introduced. Furthermore, we obtain new sufficient solutions containing cross-kink, periodic-kink, multiwaves, and solitary wave solutions. From the acquired results, it can be concluded that the procedures followed in this analysis can be implemented in a simple and straightforward manner to create new exact solutions of a lot of other nonlinear partial differential equations in terms of Hirota operator.

Data Availability

The datasets supporting the conclusions of this article are included in the article.

Conflicts of Interest

The author declares that he has no conflicts of interest.

References

[1] X. J. Yang and J. A. Tenreiro Machado, "A new fractal nonlinear Burgers' equation arising in the acoustic signals propagation," *Mathematical Methods in the Applied Sciences*, vol. 42, no. 18, pp. 7539–7544, 2019.

[2] H. M. Baskonus and H. Bulut, "Exponential prototype structures for (2+1)-dimensional Boiti-Leon-Pempinelli systems in mathematical physics," *Waves in Random and Complex Media*, vol. 26, no. 2, pp. 189–196, 2016.

[3] G. Zhou, S. Long, J. Xu et al., "Comparison analysis of five waveform decomposition algorithms for the airborne LiDAR echo signal," *Ieee Journal of Selected Topics in Applied Earth Observations and Remote Sensing*, vol. 14, pp. 7869–7880, 2021.

[4] K. Wickramasinghe, "The use of deep data locality towards a hadoop performance analysis framework," *International Journal of Communication and Computer Technologies*, vol. 8, no. 1, pp. 5–8, 2020.

[5] H. Wang, X. Wu, X. Zheng, and X. Yuan, "Virtual voltage vector based model predictive control for a nine-phase open-end winding PMSM with a common DC bus," *IEEE Transactions on Industrial Electronics*, vol. 69, no. 6, pp. 5386–5397, 1982.

[6] DR. S. Srinivasareddy, DR. Y. V. Narayana, and DR. D. Krishna, "Sector beam synthesis in linear antenna arrays using social group optimization algorithm," *National Journal Of Antennas And Propagation*, vol. 3, no. 2, pp. 6–9, 2021.

[7] X. G. Geng and Y. L. Ma, "N-soliton solution and its wronskian form of a (3+1)-dimensional nonlinear evolution equation," *Physics Letters*, vol. 369, no. 4, pp. 285–289, 2007.

[8] A. Mohammadzadeh, O. Castillo, S. S. Band, and A. Mosavi, "A novel fractional-order multiple-model type-3 fuzzy control for nonlinear systems with unmodeled dynamics," *International Journal of Fuzzy Systems*, vol. 23, no. 6, pp. 1633–1651, 2021.

[9] A. Oleinik, A. Kapitanov, I. Alexandrov, and A. Tatarkanov, "Calculation methodology for geometrical characteristics of the forming tool for rib cold rolling," *Journal of Applied Engineering Science*, vol. 18, no. 2, pp. 292–300, 2020.

[10] S. S. Band, I. Al-Shourbaji, H. Karami, S. Karimi, J. Esfandiari, and A. Mosavi, "Combination of group method of data handling (GMDH) and computational fluid dynamics (CFD) for prediction of velocity in channel intake," *Applied Sciences*, vol. 10, no. 21, p. 7521, 2020.

[11] F. Aslanova, "A comparative study of the hardness and force analysis methods used in truss optimization with meta-heuristic algorithms and under dynamic loading," *Journal of Research in Science, Engineering and Technology*, vol. 8, no. 1, pp. 25–33, 2020.

[12] B. Q. Li and Y. L. Ma, "Extended generalized Darboux transformation to hybrid rogue wave and breather solutions for a nonlinear Schrödinger equation," *Applied Mathematics and Computation*, vol. 386, Article ID 125469, 2020.

[13] X. W. Yan, "Lax pair, Darboux-dressing transformation and localized waves of the coupled mixed derivative nonlinear Schrödinger equation in a birefringent optical fiber," *Applied Mathematics Letters*, vol. 107, Article ID 106414, 2020.

[14] C. Della Volpe and S. Siboni, "From van der Waals equation to acid-base theory of surfaces," *A chemical-mathematical journey. REVIEWS OF ADHESION AND ADHESIVES*, vol. 10, no. 1, pp. 47–97, 2022.

[15] X. Liu, G. Zhang, J. Li et al., "Deep learning for Feynman's path integral in strong-field time-dependent dynamics," *Physical Review Letters*, vol. 124, no. 11, Article ID 113202, 2020.

[16] Y. Yang and Y. Zhu, "Darboux–Bäcklund transformation, breather and rogue wave solutions for Ablowitz-Ladik equation," *Optik*, vol. 217, Article ID 164920, 2020.

[17] R. Hirota, *The Direct Method in Soliton Theory*, Cambridge University Press, Cambridge, UK, 2004.

[18] K. S. Nisar, O. A. Ilhan, S. T. Abdulazeez, J. Manafian, S. A. Mohammed, and M. S. Osman, "Novel multiple soliton solutions for some nonlinear PDEs via multiple Exp-function method," *Results in Physics*, vol. 21, Article ID 103769, 2021.

[19] Y. P. Xu, P. Ouyang, S. M. Xing, L. Y. Qi, M. khayatnezhad, and H. Jafari, "Optimal structure design of a PV/FC HRES using amended Water Strider Algorithm," *Energy Reports*, vol. 7, pp. 2057–2067, 2021.

[20] J. Wei, Z. Xie, W. Zhang, X. Luo, Y. Yang, and B. Chen, "Experimental study on circular steel tube-confined reinforced UHPC columns under axial loading," *Engineering Structures*, vol. 230, Article ID 111599, 2021.

[21] H. Huang, M. Huang, W. Zhang, and S. Yang, "Experimental Study of Predamaged Columns Strengthened by HPFL and BSP under Combined Load Cases," *Structure and Infrastructure Engineering*, vol. 17, pp. 1–18, 2020.

[22] Z. Alam, L. Sun, C. Zhang, and B. Samali, "Influence of seismic orientation on the statistical distribution of nonlinear seismic response of the stiffness-eccentric structure," *Structures*, vol. 39, pp. 387–404, 2022.

[23] H. Cheng, L. Sun, Y. Wang, and X. Chen, "Effects of actual loading waveforms on the fatigue behaviours of asphalt mixtures," *International Journal of Fatigue*, vol. 151, Article ID 106386, 2021.

[24] G. Zhou, R. Deng, X. Zhou et al., "Gaussian inflection point selection for LiDAR hidden echo signal decomposition," *IEEE Geoscience and Remote Sensing Letters*, vol. 19, pp. 1–5, 2022.

[25] H. Cheng, L. Liu, and L. Sun, "Bridging the gap between laboratory and field moduli of asphalt layer for pavement design and assessment: a comprehensive loading frequency-based approach," *Frontiers of Structural and Civil Engineering*, vol. 16, no. 3, pp. 267–280, 2022.

[26] H. Huang, M. Huang, W. Zhang, S. Pospisil, and T. Wu, "Experimental investigation on rehabilitation of corroded RC columns with BSP and HPFL under combined loadings," *Journal of Structural Engineering*, vol. 146, no. 8, p. 2020.

[27] G. Zhou, W. Li, X. Zhou et al., "An innovative echo detection system with STM32 gated and PMT adjustable ga in for airborne LiDAR," *International Journal of Remote Sensing*, vol. 42, no. 24, pp. 9187–9211, 2021.

[28] W. X. Ma, Y. Zhou, and R. Dougherty, "Lump-type solutions to nonlinear differential equations derived from generalized

bilinear equations," *International Journal of Modern Physics B*, vol. 30, no. 28n29, Article ID 1640018, 2016.
[29] J. Lü, S. Bilige, X. Gao, Y. Bai, and R. Zhang, "Abundant lump solutions and interaction phenomena to the kadomtsev-petviashvili-benjamin-bona-mahony equation," *Journal of Applied Mathematics and Physics*, vol. 6, no. 8, pp. 1733–1747, 2018.
[30] J. Manafian, "An optimal Galerkin-homotopy asymptotic method applied to the nonlinear second-order bvps," *Proceedings of the Institute of Mathematics and Mechanics*, vol. 47, pp. 156–182, 2021.
[31] H. Ma, Q. Cheng, and A. Deng, "Solitons, breathers, and lump solutions to the (2+1)-dimensional generalized calogero-bogoyavlenskii-schiff equation," *Complexity*, pp. 1–10, Article ID 7264345, 2021.
[32] W. X. Ma, "Lump solutions to the kadomtsev-petviashvili equation," *Physics Letters A*, vol. 379, no. 36, pp. 1975–1978, 2015.
[33] J. Y. Yang and W. X. Ma, "Lump solutions to the bKP equation by symbolic computation," *International Journal of Modern Physics B*, vol. 30, Article ID 1640028, 2016.
[34] R. M. Miura, C. S. Gardner, and M. D. Kruskal, "Korteweg-de Vries equation and generalizations. II. Existence of conservation laws and constants of motion," *Journal of Mathematical Physics*, vol. 9, no. 8, pp. 1204–1209, 1968.
[35] J. Manafian, B. Mohammadi-Ivatloo, and M. Abapour, "Lump-type solutions and interaction phenomenon to the (2+1)-dimensional Breaking Soliton equation," *Applied Mathematics and Computation*, vol. 356, pp. 13–41, 2019.
[36] J. Manafian and M. Lakestani, "Lump-type solutions and interaction phenomenon to the bidirectional Sawada-Kotera equation," *Pramana*, vol. 92, no. 3, p. 41, 2019.
[37] R. M. Miura, "A derivation of Gardner's equation," *Methods and Applications of Analysis*, vol. 4, no. 2, pp. 134–140, 1997.
[38] B. G. Konopelchenko, "Inverse spectral transform for the (2+1)-dimensional Gardner equation," *Inverse Problems*, vol. 7, no. 5, pp. 739–753, 1991.
[39] G. F. Yu and H. W. Tam, "On the (2+1)-dimensional Gardner equation: determinant solutions and pfaffianization," *Journal of Mathematical Analysis and Applications*, vol. 330, no. 2, pp. 989–1001, 2007.
[40] A. M. Wazwaz, "New solitons and kink solutions for the Gardner equation," *Communications in Nonlinear Science and Numerical Simulation*, vol. 12, no. 8, pp. 1395–1404, 2007.
[41] T. Xu, B. Tian, H. Q. Zhang, and J. Li, "Integrable decompositions for the (2 + 1)-dimensional Gardner equation," *Zeitschrift für Angewandte Mathematik und Physik*, vol. 61, no. 2, pp. 293–308, 2010.
[42] Y. K. Liu and B. Li, "Nonlocal symmetry and exact solutions of the (2+1)-dimensional Gardner equation," *Chinese Journal of Physics*, vol. 54, no. 5, pp. 718–723, 2016.
[43] X. Wang and X. G. Geng, "N -soliton solution and soliton resonances for the (2+1)-dimensional inhomogeneous gardner equation," *Communications in Theoretical Physics*, vol. 68, no. 2, p. 155, 2017.
[44] M. Kumar and D. V. Tanwar, "On lie symmetries and invariant solutions of (2+1)-dimensional Gardner equation," *Communications in Nonlinear Science and Numerical Simulation*, vol. 69, pp. 45–57, 2019.
[45] H. M. Baskonus, T. A. Sulaiman, and H. Bulut, "Bright, dark optical and other solitons to the generalized higher-order NLSE in optical fibers," *Optical and Quantum Electronics*, vol. 50, no. 6, pp. 253–312, 2018.
[46] R. Silambarasan, H. M. Baskonus, and H. Bulut, "Jacobi elliptic function solutions of the double dispersive equation in the Murnaghan's rod," *The European Physical Journal Plus*, vol. 134, no. 3, pp. 125–122, 2019.
[47] H. M. Baskonus, "Complex surfaces to the fractional (2+1)-dimensional Boussinesq dynamical model with the local M-derivative," *The European Physical Journal Plus*, vol. 134, no. 7, pp. 322–410, 2019.
[48] G. Yel and H. M. Baskonus, "Solitons in conformable time-fractional Wu-Zhang system arising in coastal design," *Pramana - Journal of Physics*, vol. 93, no. 4, pp. 57–10, 2019.
[49] M. Goyal, H. Mehmet Baskonus, and A. Prakash, "An efficient technique for a time fractional model of lassa hemorrhagic fever spreading in pregnant women," *The European Physical Journal Plus*, vol. 134, no. 10, pp. 482–510, 2019.
[50] J. Manafian, O. A. Ilhan, and A. Alizadeh, "Periodic wave solutions and stability analysis for the KP-BBM equation with abundant novel interaction solutions," *Physica Scripta*, vol. 95, no. 6, Article ID 065203, 2020.
[51] J. Manafian, B. Mohammadi Ivatloo, and M. Abapour, "Breather wave, periodic, and cross-kink solutions to the generalized Bogoyavlensky-Konopelchenko equation," *Mathematical Methods in the Applied Sciences*, vol. 43, no. 4, pp. 1753–1774, 2019.
[52] M. Ozisik, M. Cinar, A. Secer, and M. Bayram, "Optical solitons with Kudryashov's sextic power-law nonlinearity," *Optik*, vol. 261, Article ID 169202, 2022.
[53] M. Cinar, A. Secer, M. Ozisik, and M. Bayram, "Derivation of optical solitons of dimensionless Fokas-Lenells equation with perturbation term using Sardar sub-equation method," *Optical and Quantum Electronics*, vol. 54, no. 7, p. 402, 2022.
[54] I. Onder, M. Cinar, A. Secer, and M. Bayram, "Analytical solutions of simplified modified Camassa-Holm equation with conformable and M-truncated derivatives: a comparative study," *Journal of Ocean Engineering and Science*, 2022.
[55] I. Onder, M. Cinar, A. Secer, and M. Bayram, "Soliton solutions of (2+1) dimensional Heisenberg ferromagnetic spin equation by the extended rational sine-cosine and sinh-cosh method," *International Journal of Algorithms, Computing and Mathematics*, vol. 7.
[56] M. Cinar, I. Onder, A. Secer, T. A. Sulaiman, A. Yusuf, and M. Bayram, "Optical solitons of the (2+1)-dimensional Biswas–Milovic equation using modified extended tanh-function method," *Optik*, vol. 245, Article ID 167631, 2021.
[57] M. I. Asjad, W. A. Faridi, K. M. Abualnaja, A. Jhangeer, H. Abu-Zinadah, and H. Ahmad, "The fractional comparative study of the non-linear directional couplers in non-linear optics," *Results in Physics*, vol. 27, Article ID 104459, 2021.
[58] A. Jhangeer, W. A. Faridi, M. I. Asjad, and A. Akgül, "Analytical study of soliton solutions for an improved perturbed Schrödinger equation with Kerr law non-linearity in non-linear optics by an expansion algorithm," *Partial Differential Equations in Applied Mathematics*, vol. 4, Article ID 100102, 2021.
[59] W. A. Faridi, M. I. Asjad, and A. Jhangeer, "The fractional analysis of fusion and fission process in plasma physics," *Physica Scripta*, vol. 96, no. 10, Article ID 104008, 2021.
[60] A. Jhangeer, H. Rezazadeh, and A. Seadawy, "A study of travelling, periodic, quasiperiodic and chaotic structures of perturbed Fokas-Lenells model," *Pramana*, vol. 95, no. 1, 2021.
[61] M. M. A. Khater, A. Jhangeer, H. Rezazadeh, L. Akinyemi, M. A. Akbar, and M. Inc, "Propagation of new dynamics of longitudinal bud equation among a magneto-electro-elastic

round rod," *Modern Physics Letters B*, vol. 35, Article ID 2150381, 2021.

[62] S. Khaliq, A. Ullah, S. Ahmad, A. Akgül, A. Yusuf, and T. A. Sulaiman, "Some novel analytical solutions of a new extended (2+ 1)-dimensional Boussinesq equation using a novel method," *Journal of Ocean Engineering and Science*, .

[63] S. Ahmad, A. Ullah, A. Akgül, and F. Jarad, "A hybrid analytical technique for solving nonlinear fractional order PDEs of power law kernel: application to KdV and Fornberg-Witham equations," *AIMS Mathematics*, vol. 7, no. 5, pp. 9389–9404, 2022.

[64] S. Ahmad, A. Ullah, A. Akgül, and M. De la Sen, "A novel homotopy perturbation method with applications to nonlinear fractional order KdV and burger equation with exponential-decay kernel," *Journal of Function Spaces*, vol. 202111 pages, Article ID 8770488, 2021.

[65] Y. S. Özkan and E. Yaşar, "Breather-type and multi-wave solutions for (2+1)-dimensional nonlocal Gardner equation," *Applied Mathematics and Computation*, vol. 390, Article ID 125663, 2021.